ABSTRACT

MILLER, IAN JAMES. Iterative Library Subtraction Method for Determining the Contribution of Background Radiation. (Under the direction of Dr. Robin P. Gardner).

The analysis of gamma ray spectra is a common task facing many in both academic and industrial capacities. A widely known method for evaluating spectra of interest is the library least-squares technique. This method, while very accurate, requires the user to have the spectral shape of all radioisotopes involved in the unknown spectrum. If a library is missing, the calculated amounts of each source will be incorrect. This work proposes a method to apply the principles of spectrum stripping to the unknown spectrum being operated on, with the aim of determining the spectral shape of any missing libraries. This will be done by subtracting each known library from the unknown spectrum with a magnitude determined by a fit to a peak found in both the library and the unknown. The subtraction will continue until the peak under consideration has been removed from the spectrum. The next known library will be applied to the residual spectrum, and so on until all known libraries have been removed. The final residual spectrum is subjected to a threshold method to removed noise; it can then be used as a library describing other sources of radiation present in the system. This method produced library spectra that very closely fit to unaccounted for background libraries in several different unknown spectra. The use of these calculated background libraries in a library least-squares fit with the known libraries resulted in more accurate results in all tested spectra. The proposed method could improve the library least-squares technique significantly, particularly in low energy applications. The ability to produce a background library without needing to take a separate spectrum could save valuable time and effort for applications where it is needed.

Iterative Library Subtraction Method for Determining the Contribution of Background Radiation

by
Ian James Miller

A thesis submitted to the Graduate Faculty of
North Carolina State University
in partial fulfillment of the
requirements for the degree of
Master of Science

Nuclear Engineering

Raleigh, North Carolina

2015

APPROVED BY:

_____	_____
Dr. Robin Gardner Committee Chair	Dr. Yousry Azmy
_____	
Dr. Ralph Smith	

DEDICATION

To all of those in my life that have allowed me to get to this point; none of this would be possible without your support.

BIOGRAPHY

Ian James Miller was born in Cartersville, GA in 1990 to Dwight and Karen Miller. Being born into a family with two engineers for parents, it did not take long for science to become a primary pursuit. During his high school years he was fortunate to attend a technical conference known as the Air Operated Valve Users Group (AUG) where he was able to meet several nuclear engineering professionals. Conversing with them about their time at nuclear power plants or in the nuclear navy, Ian developed an interest in the nuclear sciences. After graduating from Russell High School in 2008, Ian enrolled at the University of Tennessee-Knoxville in the nuclear engineering program. He graduated from the honors nuclear engineering program summa cum laude in 2012, and decided to pursue graduate studies in nuclear engineering at North Carolina State University. He is currently working on completing his master's degree and entering the nuclear workforce.

ACKNOWLEDGMENTS

I'd like to thank my parents, whose guidance has always steered me truly,

My classmates, who made the hard times easier to bear,

My fellow group members at CEAR, whose expertise made this work happen,

And Dr. Gardner, who gave my graduate studies a purpose and direction.

TABLE OF CONTENTS

LIST OF TABLES

LIST OF FIGURES

LIST OF EQUATIONS

Introduction

The analysis of gamma spectra to determine the elemental composition of target material is a widely used technique. It has the advantage of being non-destructive, and can be induced in target materials that are not naturally radioactive via neutron activation. Through the use of pre-generated libraries and techniques such as single peak analysis, spectrum stripping, or library least squares (LLS) estimations of elemental compositions can be made. Single peak analysis, while extremely useful for applications using very high resolution detectors, can fall short in situations where the use of lower resolution detectors is warranted. The use of elemental library based techniques such as spectrum stripping or library least squares allows for the use of the information contained across the entire collected spectrum rather than relying on peak data alone. That is not to say that these library based methods have no weaknesses. The pre-generated libraries required by these methods need to be obtained by either time consuming experimental means or computationally heavy Monte Carlo programming. Assuming those hurdles can be bypassed, there remains a potential pitfall: that the libraries generated do not cover all sources of radiation present in the collected unknown spectrum. The composition of the libraries generated to describe a target unknown material is driven by past operating experience and user input; there is potential for a source of radiation to not be accounted for due to shifting natural background or accidental activation during the neutron activation of a target material. Previous attempts have been made to use the residuals from both library least squares and spectrum stripping to determine the identity of missing libraries, with a fair amount of success. However the shape of the missing libraries cannot be obtained by these methods as employed; the peak location

and shape can be extracted but the shape of the continuum often does not agree with the residuals. This requires a return to the methods used to generate the original libraries. This can be very time consuming for experimental libraries, assuming that the missing library is something that can be isolated. For libraries generated through computational means, it may not be possible to simulate the discovered library, particularly if natural radiation is the cause. Therefore, methods that can identify a missing library in a library based approach as well as determine the missing library's shape would be of value for the field of gamma spectroscopy.

Radioactive Decay

The basics of radioactive decay described in the following chapters have been sourced from *Radiation Detection and Measurement* (Knoll, 2010) and *Introductory Nuclear Physics* (Krane, 1988). The phenomenon of radioactive decay was first observed by Antoine Henri Becquerel in 1896. It was noted three years later that this emission of energy is not constant; instead the rate of this decay decreases exponentially with time. This observation leads to the formation of the exponential law of decay, shown below in Equation 1:

Equation 1: Exponential Decay Law

$$N(t) = N_0 e^{-\lambda t}$$

Where $N(t)$ is the number of atoms remaining after time t, N_0 is the number of atoms initially, and λ is the radioactive decay constant, described by Equation 2.

Equation 2: Radioactive Decay Constant

$$\lambda = -\frac{(dN/dt)}{N}$$

These equations were formulated to take into account two important observations about radioactive decay: That radioactivity represents changes in the individual atoms of a sample rather than a change in the sample as a whole, and that the decay is statistical in nature. This means that it is impossible to know when an individual atom will disintegrate.

Statistical Considerations for Radiation Measurement

Radioactive decay is a random process. As a result, any measurement taken of a radioactive decay process will be affected by some degree of statistical fluctuation. Given a constant probability *p* of "success" or decay, the most general model that can be applied to a radiation counting experiment is the binomial distribution. However, this model is cumbersome to use for this application as the number of nuclei considered is always very large. Assuming that the probability of decay is small for an individual atom and that this probability is constant it can be shown that the binomial distribution can be simplified to the Poisson distribution, shown in Equation 3 below, where *x* is the number of counts observed in a given time period, $\bar{x}$ is the average number of counts observed in that time period, and *P(x)* is the probability of observing exactly *x* number of counts in the given time period.

Equation 3: Poisson distribution

$$P(x) = \frac{(\bar{x})^x e^{-\bar{x}}}{x!}$$

It can be shown that this distribution has a very simple expression for variance in a single measurement, found in Equation 4.

Equation 4: Poisson distribution variance

$$\sigma^2 = x$$

This is an important result because it directly relates the number of counts collected during the measurement of an unknown to the expected variance in the final result; i.e. the more counts collected the smaller the fractional uncertainty will be. A further simplification to the Poisson model can be made if the assumption is made that the average number of successes is large (greater than 25). The result of this assumption is the Gaussian distribution, shown below.

Equation 5: Gaussian distribution

$$P(x) = \frac{1}{\sqrt{2\pi\bar{x}}} e^{-\frac{(x-\bar{x})^2}{2\bar{x}}}$$

The Gaussian distribution is often more convenient that the Poisson distribution as it is a continuous function rather that a discrete one.

Radioactive Decay Types

A nucleus seeks to decay because it is unstable. This can occur for a number of reasons, such as a proton/neutron imbalance or currently existing in an excited state. There are several decay types that nuclei will employ to reach a more stable state. Some examples are alpha (α), beta (β), and gamma (γ) decay.

Alpha Decays

When a nucleus undergoes alpha decay the unstable nucleus emits an alpha particle in order to reach a more stable isobar. The alpha particle was shown to be a helium nucleus by Rutherford, and is a good candidate for this process due to its high binding energy. This

maximizes the kinetic energy the decay can release, which makes the entire process more favored. The alpha decay process is shown symbolically in Equation 6 below:

Equation 6: Alpha Decay

$$ {}^{A}_{Z}X_{N} \underset{\alpha}{\rightarrow} {}^{A-4}_{Z-2}Y_{N-2} + {}^{4}_{2}He_{2} $$

Where *A* is the mass number of the atom, *Z* is the atomic number of the atom, and *N* is the neutron number of the atom.

Beta Decays

The goal for beta decay is the same as in alpha decay, but the particle emitted differs. Instead of nucleons, beta decay emits either an electron or positron. Cases where an electron is emitted are known as beta minus (β-) decays, positron emission is known as beta plus (β+) decays. These processes are shown symbolically in Equation 7 and Equation 8.

Equation 7: Beta Minus Decay

$$ {}^{A}_{Z}X_{N} \underset{\beta^{-}}{\rightarrow} {}^{A}_{Z+1}Y_{N-1} $$

Equation 8: Beta Plus Decay

$$ {}^{A}_{Z}X_{N} \underset{\beta^{+}}{\rightarrow} {}^{A}_{Z-1}Y_{N+1} $$

In both decays, the emission of the beta particle is accompanied by a neutrino. This neutrino affects the kinetic energy of the beta particle but has no charge.

Gamma Decay

It is fairly uncommon for a nuclear reaction or decay to leave the daughter nucleus in its ground state. Far more often the end result is an excited daughter nucleus. The primary method for de-exciting is through gamma decay. While all forms of radioactive decay have practical applications, those that rely on particle emission rather than energy emission have

limitations. The primary problem with using alpha and beta particles is that they are quickly stopped in matter, even air. This limits the range at which the particles can even be detected. Gamma rays are much more suitable for detection. They can travel much further than the heavy particles while retaining the energy they were emitted with. If they can be observed in a suitable manner, it may be possible to determine what isotope emitted them.

Radiation Interaction with Matter

The task of radiation detection would be greatly simplified if all radiation was emitted in the visual spectrum. Sadly that is not the case. In order to determine anything about characteristic radiation an interaction with matter that results in something measureable must occur. This chapter will describe the ways radiation interacts with matter; suitable detection materials will be discussed in later chapters.

Gamma Ray Interactions

Gamma rays are capable of interacting with matter in a myriad of different ways. Three of these mechanisms are important for radiation detection, namely photoelectric absorption, Compton scattering, and pair production. Each functions very differently and is predominant at different energy ranges.

Photoelectric Absorption

In photoelectric absorption, a gamma ray is absorbed by an atom in the target material. In its place a photoelectron is ejected. The energy of this photoelectron is determined by the energy of the absorbed gamma ray, less the binding energy of the ejected

electron. This relationship is shown in Equation 9 below, where E_{e-} is the energy of the ejected photoelectron, E_γ is the energy of the incident gamma ray, and E_b is the binding energy of the electron before ejection.

Equation 9: Photoelectric Absorption Photoelectron Energy

$$E_{e-} = E_\gamma - E_b$$

This is an important interaction mechanism as it is the only one out of the three primary interaction mechanisms that results in the complete capture of all the incident energy. Photoelectric absorption generally has high cross sections at gamma ray energies from 0-300 KeV and for materials with a high Z number.

Compton Scattering

As convenient as it would be for all interaction events to be photoelectric absorption, many gamma ray energies are much greater than the primary energy range for that interaction. As incident photon energy increases, the probability of Compton scattering increases as well. This process, instead of interacting with the entire atom as in photoelectric absorption, is considered to take place between one electron in the target material and the incoming gamma ray. The gamma ray is scattered at an angle θ off of its original path. A portion of the scattering gamma rays energy is transferred to the struck electron, which is known as the recoil electron. The relationship between the initial (E_γ) and final (E_γ') gamma ray energies is shown in Equation 10, where m_0c^2 is the rest mass of the electron (0.511 MeV). Equation 11 shows the relationship between the energy change of the gamma ray and the energy imparted to the recoil electron.

Equation 10: Compton Scattering

$$E'_\gamma = \frac{E_\gamma}{1 + \frac{E_\gamma}{m_0 c^2}(1 - \cos\theta)}$$

Equation 11: Compton Scattered Recoil Electron Energy

$$E_{e-} = E_\gamma - E'_\gamma$$

Depending on the scattering angle this type of interaction can result in a large amount of energy imparted to the recoil electron or none at all. This mechanism is present at all energies, but is the predominant interaction method for gamma rays of energies between 0.5-4 MeV.

Pair Production

Pair production is a process by which a gamma ray with sufficient energy enters the coulomb field of an atom's nucleus and in changed into an electron-positron pair. The energy required for this to happen is twice the rest mass energy of an electron, 1.022 MeV. The electron created will lose its energy as it travels through the medium until it stops; the positron will encounter another electron in the target material and annihilate. This is a process where the positron and electron disappear and two gamma rays with energies equal to the mass of an electron (0.511 MeV) appear.

Neutron Interactions

For those attempting to ascertain properties of a material via gamma ray spectrum analysis, it would be convenient indeed if all materials were naturally emitting gamma rays. Fortunately for the health of all most materials are not significantly radioactive. In order to gather a gamma ray spectrum from a stable material an excited state must be induced by an

outside source. While high energy gamma rays can induce such a state, the most common mechanism for bulk material activation is through neutron bombardment. The mechanism by which the neutrons accomplish this depends greatly on the energy of the neutron at the time of the interaction.

Neutron Capture

The first mechanism for neutron activation of materials is neutron capture. This is an interaction in which a neutron is absorbed by a nucleus in the target material. After absorbing the neutron, the nucleus is left in an excited state. It is capable of de-exciting via many mechanisms, including the emission of a neutron. However the most likely de-excitation mechanism is through gamma radiation. These gamma rays are emitted at specific energies determined by the energy level scheme of the target nucleus. This is important because if the level scheme of a material is known beforehand, gamma rays of certain energies can be tied to interactions with certain nuclei. The activity of these specific gamma rays can be used to determine the amount of the nuclei present.

Elastic Scattering

Neutron capture is a very convenient interaction method for inducing gamma activity in materials where there would otherwise be none. Unfortunately neutron capture is only the dominant neutron interaction at low energies. The majority of neutron sources produce neutrons at higher energies where capture is a rare event. The neutrons must be slowed to be useful; the way that is accomplished is through elastic scattering. Elastic scattering is an interaction between an incident neutron and a nucleus. The neutron approaches the nucleus

of mass *A* with energy *E*; it is then scattered at an angle θ with energy *E'*. This interaction is described by Equation 12 below.

Equation 12: Neutron Elastic Scattering

$$\frac{E'}{E} = \frac{A^2 + 1 + 2A\cos\theta}{(A+1)^2}$$

This relationship shows that the energy lost by the incoming neutron is most heavily influenced by the mass number of the target nucleus. The heavier the nucleus, the more elastic collisions must occur to slow the neutron down to thermal energies. In practice, this is done either by using a hydrogen rich material between the neutron source and the material to be activated to minimize the number of collisions needed to thermalize the neutrons, or by using a heavier but denser material to maximize the number of interactions likely to happen within the intervening material.

Detection Systems

In order for radiation to have any practical use a system must be devised that can convert the incoming radiation into an electrical signal that can be accepted by today's signal processing equipment. This is usually done by the chaining of several signal processing components together, such as a preamplifier, amplifier, and multichannel analyzer (MCA). The most important component, however, is the radiation detector itself.

Detector Mechanisms

Simply knowing the ways in which gamma radiation interact with matter is not enough. In order to produce useful information, an event must occur that translates the

incoming gamma rays into something that can be collected by an electronic system. Fortunately, there are several mechanisms that can accomplish this. The spectra shown later in this work have all be collected by a sodium iodide (NaI) inorganic scintillator that has been doped with trace amounts of thallium iodide; the bulk of this section will explain the mechanism behind this particular detector. The reader should be aware that other systems of radiation detection exist, such as gas filled or semiconductor detectors. These detectors have different operating principles but the goal is the same: the conversion of radiation to a measureable signal.

Inorganic Scintillators

Scintillation radiation detectors seek to transform incident radiation energy into visible light, which through devices such as a photomultiplier tube can be converted into a usable electronic signal. This is done by the process of fluorescence, which is the prompt emission of visible radiation from a substance following its excitement by some means, in this case, interaction with incoming radiation.

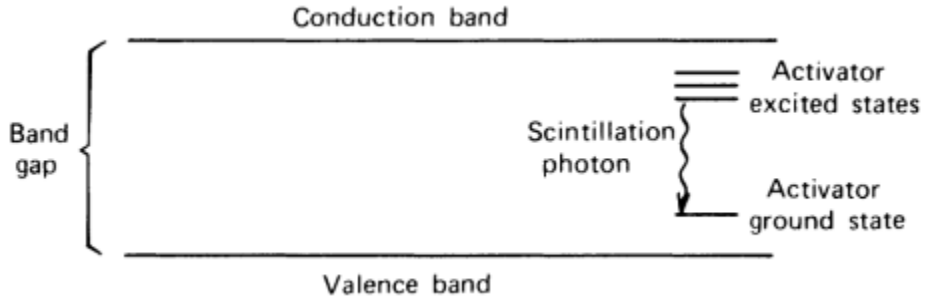

Figure 1: Inorganic Scintillation Mechanism

Figure 1 is an illustration of how the excitation process works in inorganic scintillators. The structure of the conduction and the valence energy bands depends on the crystal lattice of the scintillation material. The electrons that populate the valence band can be thought of as bound within the lattice of the crystal, while the conduction band is populated by electrons that are unbound by this structure. If a gamma ray were to interact with one of the electrons in the valence band via the mechanisms described in the previous sections it is possible for that electron to gain enough energy to jump into the conduction band. This creates a "hole", or absence of negative charge, in the valence band. This hole will be filled by an electron from the conduction band; in order for the conduction electron to make the transition to a lower energy state excess energy is emitted in the form of photons. The wavelength of these photons is dictated by the band gap. Unfortunately, in a pure crystal, the wavelength of photons emitted is outside of the visible spectrum and cannot be used as a scintillator. This can be overcome through doping the crystal with a small amount of impurities known as activators. The addition of these impurities adds energy levels to the crystal structure between the conduction an valence bands. Instead of the conduction electron losing all of its energy at once, creating a photon with an unusable wavelength, the electron can travel through the energy states of the activator on its way to the valence band. If done properly this will result in visible light that can form the basis for a scintillation detection system. However it is important to note that the light emitted from the detection crystal will not be strong enough on its own to result in a workable signal. Additional multiplication is needed if the signal generated by the scintillation of the detector is to be discernible over the electronic noise inherent to these systems.

Photomultiplier Tubes

The rise of scintillators as radiation detection systems would not have been possible without the development of the photomultiplier (PM) tube. This device not only transforms the photons produced by the scintillation crystal into electrons, it is capable of increasing the magnitude of the resulting signal without adding an undue amount of noise.

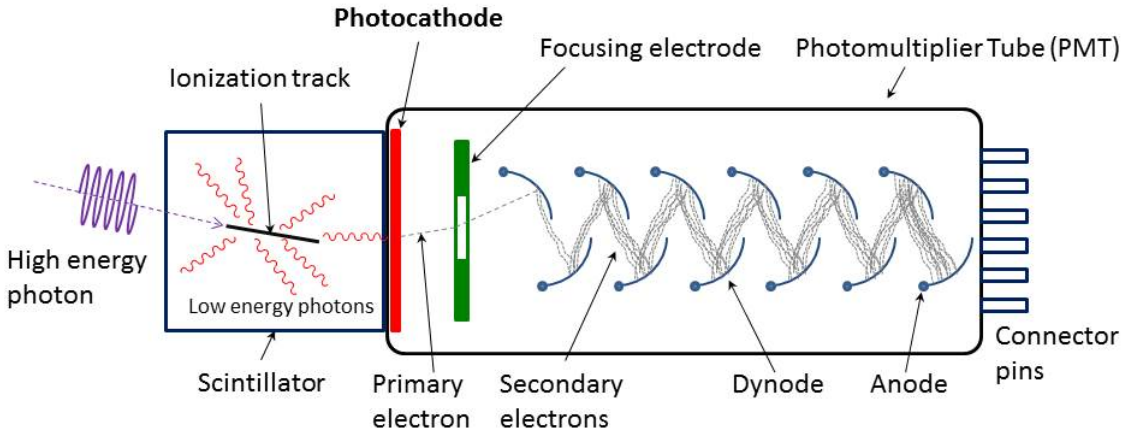

Figure 2: Photomultiplier Tube

Figure 2 above shows a simplified structure of the typical photomultiplier tube. There are two primary components within a PM tube: the photocathode and the electron multiplier. The photocathode is a negatively charged electrode that is coated in a photosensitive compound. This ensures that when the photocathode is struck by a photon of light, a photoelectron will be emitted. The electron multiplication system works by accelerating the photoelectrons produced by the photocathode. This is done by giving an electrode past the photocathode a very strong positive charge; this type of electrode is known as a dynode. The dynode is constructed so that when the original electron strikes its surface after acquiring

kinetic energy from the acceleration several more electrons will be released. This process can be repeated several times which will greatly increase the electron yield of the radiation interaction event.

Preamplifiers

The output from a detector component, regardless of mechanism, is a burst of charge liberated by the incident radiation. For the scintillation case, with would be the total number of electrons produced by the photomultiplier tube. The next device in the detection chain is most commonly a preamplifier. This component seeks to amplify the signal obtained from the detector before systemic noise clouds it. To do this, the preamplifier is placed as close to the detector as possible in the signal chain, the aim being to minimize the length of cabling between the detector and the preamplifier. The preamplifier generally provides no pulse shaping, and outputs a linear tail pulse to the next device in the detection chain. It should be noted that in general the signal obtained from a scintillation system is generally quite large compared to other methods of detection, meaning the amplification of the preamplifier is not strictly necessary. With that being said it is common practice to include a preamplifier anyway, as its use will simplify device settings further down the equipment chain.

Amplifiers

The pulses produced by a preamplifier, by design, have a very long tail. This is to ensure that all of the charge produced by the detection event is collected. However, the tail also poses a problem for electronic measurement: the information about the radiation event is carried in the amplitude of the pulse, and unless the event rate is very low, the pulses will

overlap the long tail of the previous pulse. As the time between events is random, this makes the amplitude of the pulse a bad metric for extracting event information. This problem can be solved by the use of a shaping amplifier. The amplifier shapes the pulses so that the long tails are eliminated, but the proportionality between the pulse amplitude and the charge of the radiation interaction event is preserved.

Counting systems

Once a workable pulse shape is obtained, the next task is to determine the objective of the detection system as a whole. A simple count rate can be obtained by the use of an integral discriminator, which operates by setting a voltage threshold that the pulse output by the shaping amplifier must exceed to be counted. If the user desires counting information about a specific energy range, differential discrimination can be employed. This device, known as a single channel analyzer (SCA), uses both a high and low voltage threshold. If the pulse amplitude falls between the two bounds then the pulse is recorded as a count. For applications that demand the amplitude distribution of pulses from the detector, i.e. spectral analysis, a multichannel analyzer (MCA) is needed. The simplest way to visualize how an MCA operates is to imagine several SCAs working in concert. Each SCA, or "channel", is active over a certain energy range. If a pulse falls within one of the channels covered by the MCA, a count for that specific channel is recorded. Once many events have been collected, radiation spectrum of the measured source can be obtained.

Sources of Background Radiation

A constant concern for those attempting to use gamma spectroscopy is that of background radiation. There are two main sources of background radiation, so called naturally occurring radioactive materials (NORM) and cosmic radiation (Mitchell, 2008). NORM represents materials commonly found in the earth or in building materials that naturally contain radioactive isotopes. There are three isotopes that make up the majority of NORM background sources: ^{40}K, ^{232}Th, and ^{238}U. The gamma ray energies and intensities emitted by these isotopes can be found below.

Table 1: NORM Sources of Background

Isotope	Energy (keV)	Intensity (per decay)
^{40}K	1460.75	0.1067
^{232}Th	74.81	0.105
	77.11	0.177
	238.632	0.433
	338.32	0.11257
^{208}Tl	2614.53	100
^{238}U	295.24	0.193
	351.932	0.376

Note that ^{208}Tl was included as it produces the highest energy gamma ray in the ^{232}Th decay chain. In fact, this gamma from 208Tl is the highest energy gamma ray produced by naturally occurring materials; this limits the contribution of NORM sources to a collected spectrum to a range of less than 2.61 MeV.

In addition to NORM isotopes, cosmic radiation can also provide a source of background. This type of background is produced when cosmic radiation interacts with the earth's atmosphere, creating secondary radiation such as mesons, electrons, protons, neutrons, and photons with energies that extend into the hundreds of MeV range. The high energies this type of background is capable of makes for a much different spectral shape than NORM sources. NORM sources essentially look like any other gamma ray source, with a full-energy peak and a continuum behind it. The high energy nature of cosmic radiation, however, means that few detectors have the size to completely stop an incoming particle. This means that the spectrum from cosmic radiation is much smoother than NORM, often lacking a true full energy peak.

A fairly common approach in determining the material composition of a target not naturally radioactive is to active the target with a source of neutrons. While effective, this method can also introduce new sources of background into the final spectrum that will need to be accounted for. The neutrons used to activate the target material will also activate other materials in the testing environment. A common contributor to the spectrum is the detector crystal itself, in the form of both activation and prompt gamma rays. Materials surrounding the detection setup could just as easily become activated and would need to be accounted for. Gamma rays from the neutron source could also be a contributor, depending on the type of source used.

Library Least Squares applied to Gamma Spectroscopy

The following derivation can be found in greater detail in *Analysis of Gamma-Ray Scintillation Spectra by the Method of Least Squares* (Salmon, 1961). For the purposes of derivation, it will be assumed that the multichannel analyzer used for spectrum collection has *n* channels numbered 1…*i*…*n* and the spectrum collected is the result of a source that contains *m* radionuclides. Individual libraries for these *m* radionuclides have already been obtained for the experimental geometry and detection system employed, and will be labeled 1…*j*…*m*. The count rate in channel *i* from library *j* will be denoted as a_{ij} and the total count rate in channel *i* will be denoted as b_i. Equation 13 shows the relationship between the recorded count rate and the known libraries, where x_j is the multiplier attached to library *j* and E_i is random error.

Equation 13: Channel Count Rate in Terms of Known Libraries

$$b_i = \sum_{j=1}^{m} a_{ij} x_j + E_i$$

The optimal values of x_j can be found by minimizing *R*, which is the sum of the squares of E_i. This relationship can be found in below Equation 14.

Equation 14: Sum of the Squares of E_i

$$R = \sum_{i=1}^{n} E_i^2 = \sum_{i=1}^{n} \left[b_i - \sum_{j=1}^{m} a_{ij} x_j \right]^2$$

R is minimized by performing a partial derivative with respect to x_j and setting the result equal to zero. Clearly there is one such equation for each channel in the collected spectrum, leading to a series of *m* equations labeled 1…*k*…*m* of the form shown below in Equation 15.

Equation 15: Series of Least Squares Equations

$$\sum_{j=1}^{m} x_j \sum_{i=1}^{n} a_{ik} a_{ij} = \sum_{i=1}^{n} a_{ik} b_i$$

The series of equations in Equation 15 can be written in matrix form, as shown in Equation 16.

Equation 16: Series of Least Squares Equations in Matrix Form

$$Ax = y$$

The solution to Equation 16 can be found below:

Equation 17: Solution to Least Squares Equations

$$x = A^{-1} y$$

The inverse matrix A^{-1} can be calculated manually for small values of *m*, but in the realm of spectral analysis *m* is frequently greater than 1000. This necessitates the use of computational solvers. The variance of x_j is given by Equation 18, where $[d_{jj}]^{-1}$ is the corresponding diagonal elements of the inverse matrix A^{-1}.

Equation 18: Variance of x_j

$$VAR(x_j) = \frac{E}{n-m}\left[d_{jj}\right]^{-1}$$

Using this method the best ratio of elements in the mixed source can be determined while minimizing statistical error and avoiding subjective errors. A convenient method for determining the quality of the least squares fit to the unknown data is the reduced chi-squared value, defined below in Equation 19 (Bevington, 2003):

Equation 19: Reduced Chi-Squared

$$\chi_v^2 = \frac{1}{v} \sum_{i=1}^{n} \frac{E_i^2}{\sigma_i^2}$$

Where v is the number of degrees of freedom in the dataset and σ_i^2 is the standard deviation of R. As per Equation 4, σ_i^2 can be described by the number of counts in channel i of the unknown. This process will be performed by a Levenberg–Marquardt (Marquardt, 1963) based solver known as CURMOD. CURMOD is based on techniques detailed in Bevington (Bevington, 2003).

One weakness in this method, however, is that all of the radionuclides present in the collected spectrum need to have a library associated with them. If a major contributor to the collected spectrum is not included in the least squares solution, the other known libraries will be forced to include the counts of the missing radionuclide in their computed contributions, leading to incorrect solutions. In order to demonstrate this effect, a brief example has been prepared. The author obtained several prompt gamma elemental libraries resulting from the Monte Carlo simulation of a coal analyzer prototype; specifically these libraries came from the CEARCPG code developed by Xiaogang Han (Han, 2007). The libraries chosen for this example are carbon, hydrogen, nitrogen, oxygen, and nitrogen, and can be found in Figure 3 below.

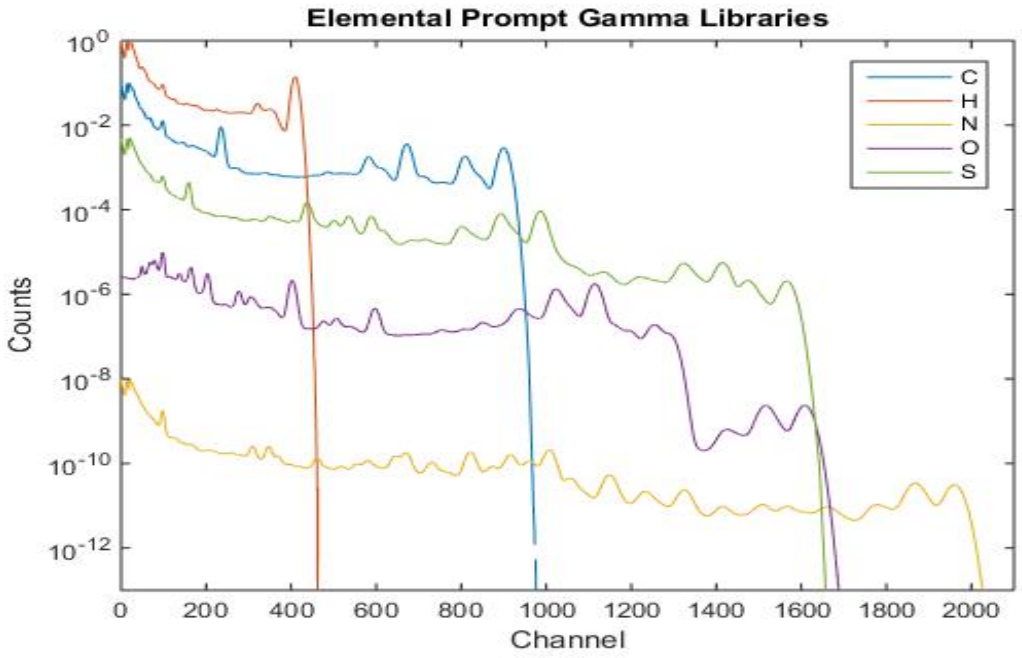

Figure 3: Elemental Prompt Gamma Libraries for LLS Example

The reader should note that the libraries in Figure 3 have been manually spaced so that the peaks present in each can be easily identified; the actual libraries have all been normalized to one. These libraries were combined in a 1:1:1:1:1 ratio to create an "unknown" spectrum for performing a library least squares (LLS) analysis on. This unknown spectrum is shown in Figure 4.

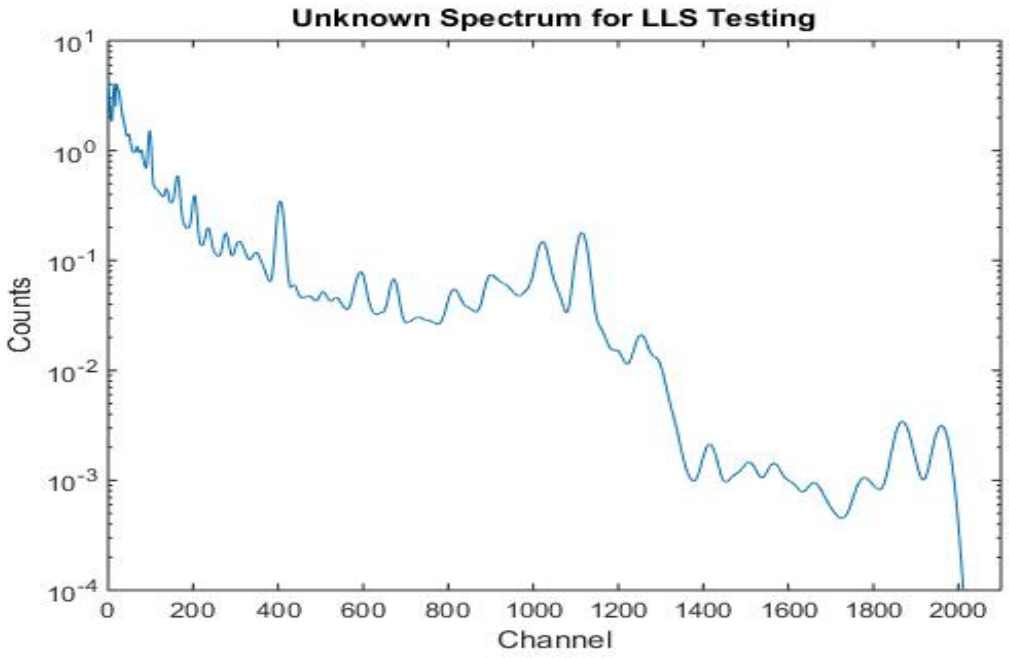

Figure 4: Example Unknown Spectrum Created by Combination of Example Libraries

A LLS fit was performed on this unknown including all five libraries using the CEARLLS code (Gardner R. , 1997); this represents the case where the libraries used in the analysis of the unknown correctly cover all of the elements present in the unknown. The results of this fit can be found in Figure 5 and Table 2. Note that an offset has been applied in Figure 5 for ease of viewing the two datasets; the magnitude of the two is the same across the entire spectrum.

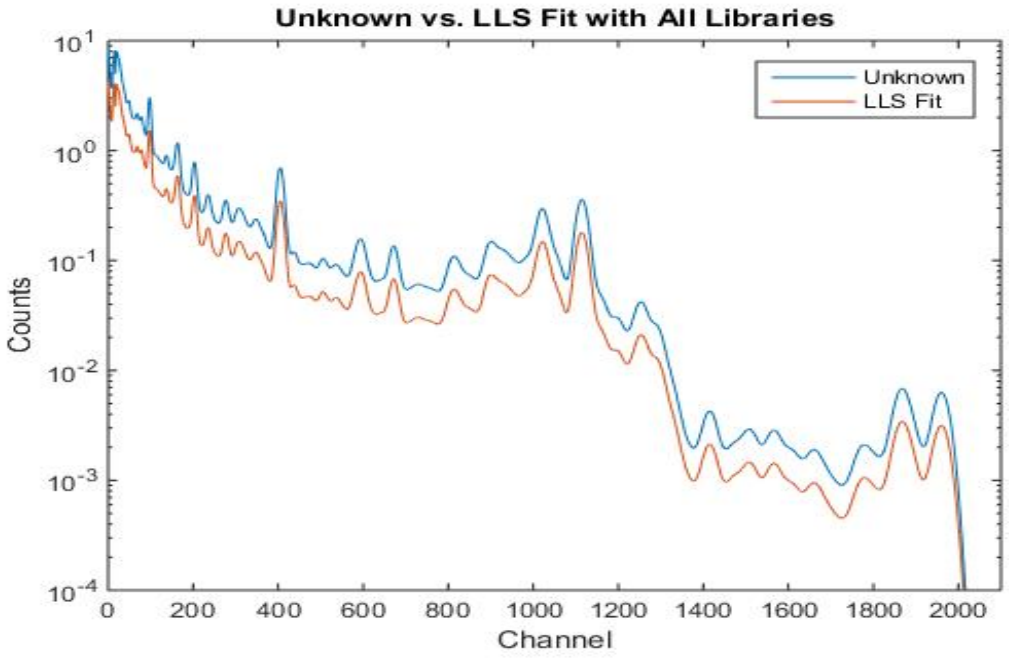

Figure 5: Unknown Spectrum vs. LLS Fit with All Libraries

Table 2: LLS Fitting Results with All Libraries Included

Library	True Library Multiplier	LLS Solved Multiplier	% Area Covered By Library
C	1	1	15.86
H	1	1	14.76
N	1	1	17.14
O	1	1	36.31
S	1	1	15.92

Clearly the fit of the libraries to the unknown results in a satisfactory fit, as was expected. Figure 6 and Table 3 below show the results of a LLS fit to the same unknown but without the oxygen library.

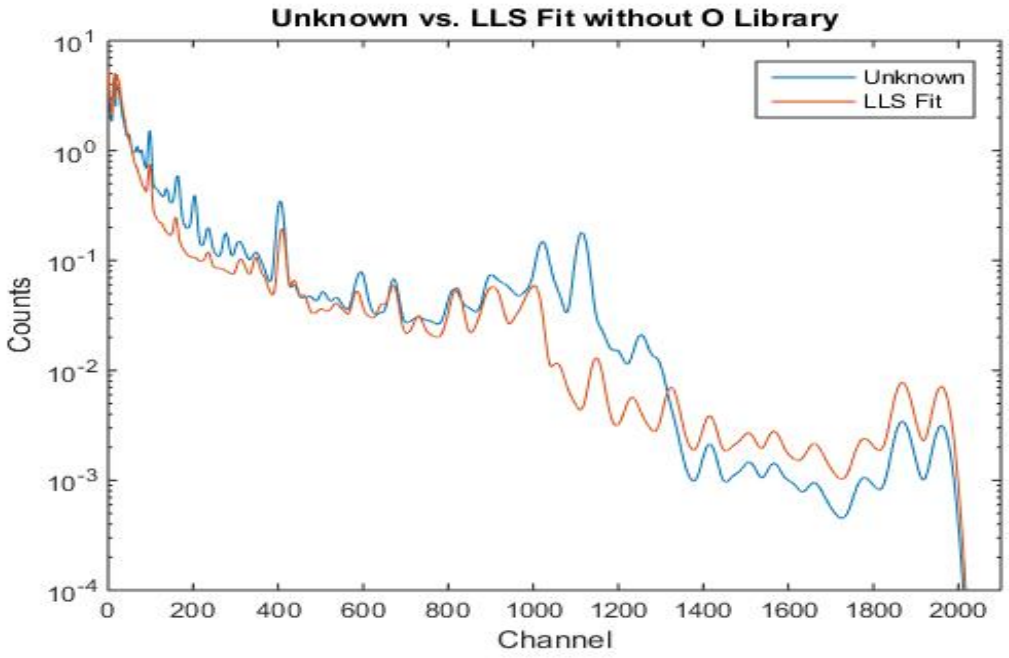

Figure 6: Unknown vs. LLS Fit without O Library

Table 3: LLS Fitting Results without O Library

Library	True Library Multiplier	LLS Solved Multiplier	% Area Covered By Library
C	1	0.392717	6.23
H	1	1.12273	16.57
N	1	2.27019	38.92
S	1	1.50377	23.94

As was to be expected, the omission of a contributing library negatively affects the library least squares solution for the unknown.

Library Generation

In order to utilize the library least squares method for spectral analysis, libraries must first be constructed. There are two primary methods for library generation: experimental and calculation. There a benefits and drawbacks to both methods.

Library Generation via Computer Generation

While there are several methods of generating libraries through computer generation, a method that has risen to prominence is the use of Monte Carlo simulation. The nature of a Monte Carlo simulation allows for the relatively easy definition of the source and detector geometry. The primary downside to using a pure Monte Carlo approach is that it is very time consuming. Each particle needs to be modeled from its "birth" within the radioactive sample to the resulting pulse of electrons from its interaction within the detector. Tracking a single gamma ray as it moves through its lifetime is fairly simple; simulating the exact response of the detector is not. A more practical approach is to use Monte Carlo to determine the extent of the full energy peak, the Compton continuum, the annihilation photons, and the x-ray escape peaks. With this data in hand, a detector response function (DRF) is applied to determine how each incident gamma ray energy will affect the detectors output. As the DRF is a relatively simple program compared to a full Monte Carlo simulation, this approach can save a significant amount of time while maintaining a high degree of accuracy. Once the incident prompt gamma ray spectra for each element in the source of interest has been simulated through Monte Carlo and the DRF has been determined, it is a fairly simple matter to determine the library for each element. Equation 20 details its usage, where C_i are the

total number of counts in channel i which have a pulse-height energy E_i, C_j are the counts incident on channel j in E_j, D_{ij} is the discretized DRF for E_j corresponding to the channel with E_i, m is the number of energy-count pairs for the element of interest and n is the total number of channels in each library DRF.

Equation 20: Detector Response Function Application

$$C_i = \sum_{j=1}^{m} C_j D_{ij}\,, i = 1, n$$

Detector Response Function Generation

There are three main methods of generating DRFs: Experimental, Monte Carlo, and Semi-empirical. The experimental method entails obtaining the response in matrix form for several monoenergetic spectra and then interpolating between the known energies to complete the entire range of energies (Furr, 1968). This method results in spectra that are closer to elemental library spectra than true DRFs, as they include detector imperfections as well as shielding in the final result. The downside is that the collection of this information is extremely time consuming and may not be practical if a very wide range of energies are required.

The Monte Carlo method (Gardner R. P., 2004) is similar to the experimental method in that it entails the collection of a large number of monoenergetic spectra and the interpolation between them; the difference is that these spectra are simulated rather than collected experimentally. While this minimizes the amount of experimental work that must be done, care must be taken to appropriately characterize the source-detector system. Additionally, any detector irregularities will not be accounted for.

The semi-empirical method (Sood, 2004) requires the determination of an analytical model for separable detector features and uses a least squares fit to a number of monoenergetic spectra to determine model parameters. This approach requires less experimental data and can be tailored for individual detectors; the problem is that very little insight can be gleaned about the actual deposition mechanics within the detector through an analysis of the analytic model. If the model does not match with experimental data, it can be difficult to determine why.

Spectrum Stripping

Spectrum Stripping was one of the first attempts to use the library concept to analyze gamma ray spectra. After the acquisition of elemental libraries that describe the composition of the unknown, the library with the highest energy peak is identified. This peak is should exist in the unknown if the libraries adequately describe the unknown and enough counting time was taken to ensure good counting statistics; assuming that it does, the library corresponding to this peak is subtracted from the entire unknown spectrum until the highest energy peak is removed from the system. Once the peak is removed, the library's contribution to the unknown is considered to be removed as well. The library with the next highest energy peak is identified, and the process repeats. This process is shown graphically in Figure 7 below.

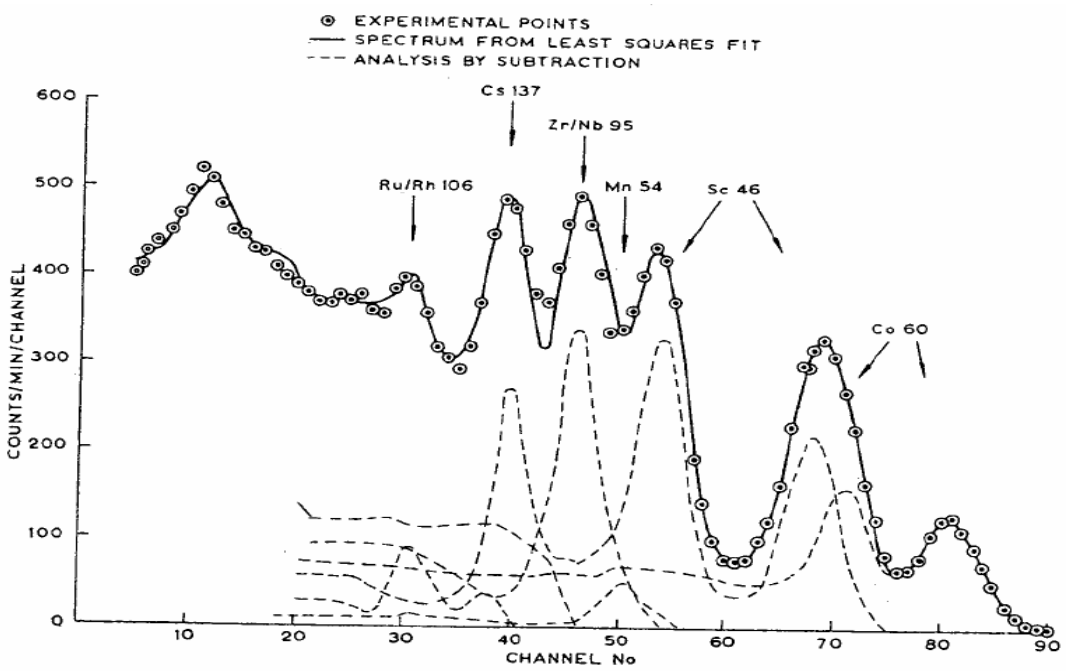

Figure 7: Spectrum Stripping via Elemental Libraries

In this figure the unknown spectrum is represented by the dotted lines; the libraries used for subtraction are shown by dashed lines. In this authors case, the metric used to determine when a peak was completely removed from the system was a least squares fit of the library peak to the corresponding peak in the unknown. The multiplier value attached to the library that produced the lowest chi squared value was applied to the entire library and subtracted from the unknown spectrum. The solid line represents the reconstruction of the unknown spectrum by summing all of the elemental libraries times their solved multipliers. Clearly the method has merit as the result is a very good fit. In more recent years, a study was done by DiNova on the use of spectrum stripping in cases where not all libraries were initially known by the user (DiNova, 2011). A test case was constructed of the combination of Cs-137, Co-60, and uranium, individually shown in Figure 8 in black, blue, and red respectively. Figure

9 shows the combination of these libraries with the addition of Poisson noise to simulate a real collected spectrum.

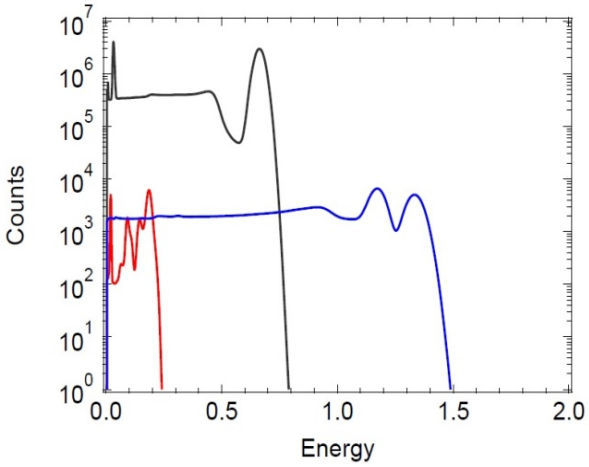

Figure 8: Spectrum Stripping Example Libraries

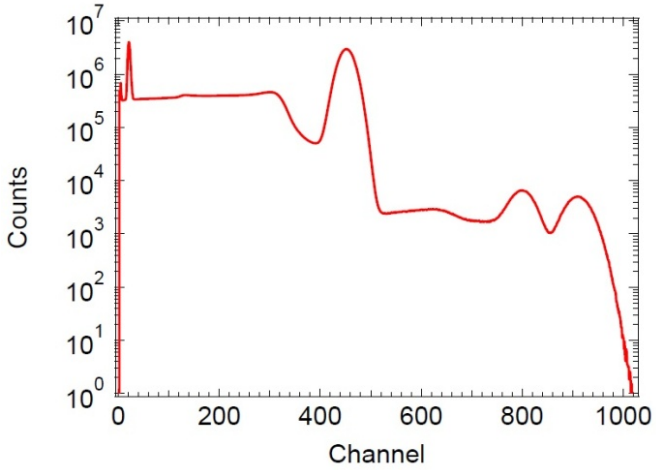

Figure 9: Unknown Spectrum for Spectrum Stripping Example

The assumption made was that the spectrum was being analyzed without the knowledge that uranium was present. The contributions of Cs-137 and Co-60 were stripped away using the methods described above, which resulted in the residuals found below in Figure 10.

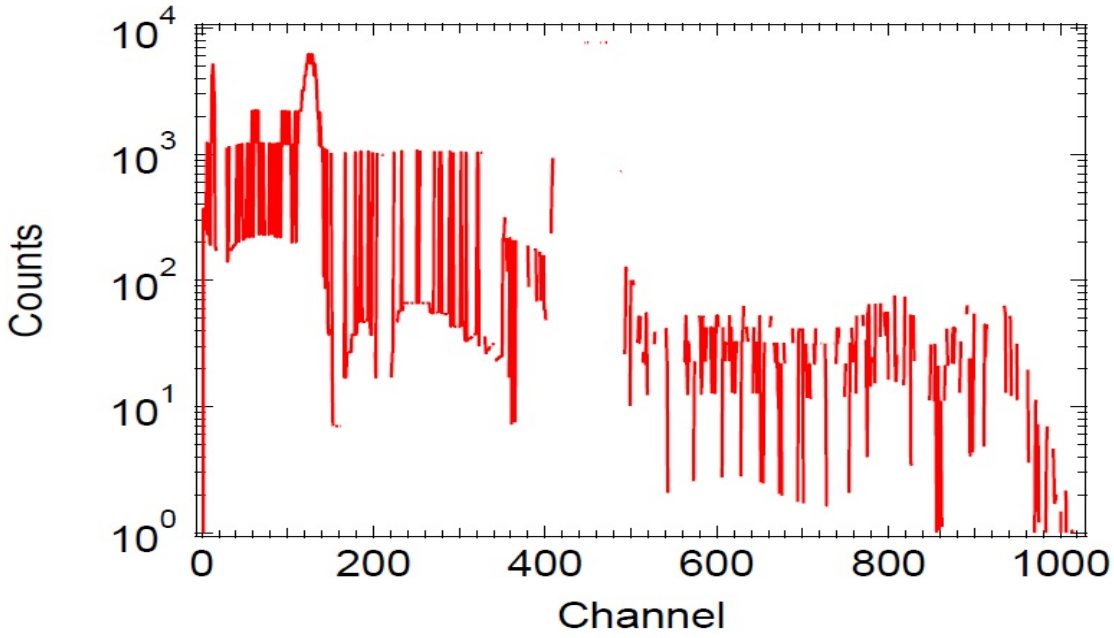

Figure 10: Spectrum Stripping Example Residuals

Clearly the analyst would recognize that something was present in the spectrum. However, if the goal of the analysis was to determine the contribution of all elements present in the unknown, the next step would be to generate a library for this newfound contributor via the methods described earlier in this work, such as by experimentation or Monte Carlo simulation. If an analysis method existed that could result in a usable library for these unknown contributors a lot of time and effort could be saved.

Iterative Subtraction Method Development

The primary problem with subtracting library spectra in the areas in which they would be most effective (i.e. areas with good counting statistics) is that in all but the most simple spectra the area with favorable counting statistics will contain contributions from other sources of radiation besides the library up for subtraction. The method of spectral stripping relied on subtracting a library until a chosen peak was essentially reduced to zero counts, with the residual spectrum representing the spectrum less the contributions across all channels of the removed library. This method will clearly not be sufficient if other contributors exist in the range of channels used to determine if the subtracting library has been removed; the magnitude of the subtraction will be far greater than the library's actual contribution to the spectrum. Therefore, a different metric for library removal needs to be defined.

Peak Fitting

In order to illustrate the problem at hand and the method used to solve it, refer to Figure 11 for an example spectrum and library set.

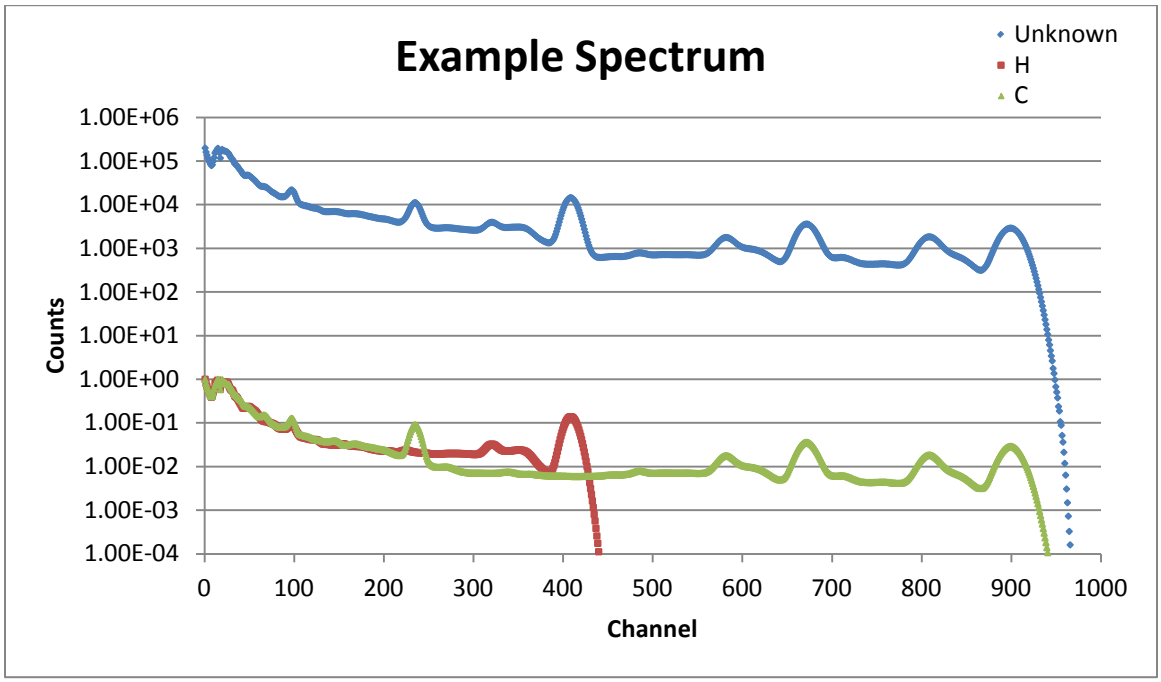

Figure 11: Test Spectrum for Method Demonstration

For this example, the unknown spectrum consists of a linear combination of the prompt gamma ray spectra of hydrogen and carbon. Traditional spectrum stripping would dictate that the first peak to be operated on would be at the far right end of the spectrum in Figure 11, removing carbon first. However, the magnitude of the hydrogen peak means that if it could be subtracted first, subsequent subtractions would be subject to far less error. To do this, the metric for complete subtraction has to be different than simply attaining zero counts across the peak in question. The first step will be to define a model that describes hydrogen's contribution across the range of the peak started at channel 380 and ending at channel 425 as well as the contribution of other sources of radiation in the same channel range. It can be shown (Routti, 1969) that a Gaussian distribution can provide a rough approximation of a photopeak in a gamma ray spectrum. There are features of the photopeak that deviate from

the Gaussian, particularly in the low energy side of the peak in the form of tailing, but in the interest of the simplest working model a Gaussian will be accurate enough. This portion of the model will describe the contribution of the library that is being subtracted from the spectrum, assuming that the peak in the unknown that corresponds to the peak in the library is not convolved with any other radioisotope peaks. Such convolution will be treated later in this work. Assuming an unconvolved peak, the other contributions across the peak range will take the form of a continuum that the library peak sits on top of; this can be reasonably approximated as a first order polynomial. The entire fitting model can be found in Equation 21 below:

Equation 21: Peak Fitting Model

$$Gaussian = a(3) * \exp\left(-\frac{\left(\mathrm{x} - \mathrm{a}(1)\right)^2}{2 * \mathrm{a}(2)^2}\right)$$

$$Polynomial = a(4) * x + a(5)$$

$$Model = Gaussian + Polynomial$$

Where *a(1)* and *a(2)* are the centroid and standard deviation of the Gaussian, respectively, and *a(3)*, *a(4)*, *a(5)* are linear constants. This model conveniently separates the spectral contribution of the library to be subtracted and all other sources of counts. As such, a new metric for the subtraction of a library emerges: if the contribution of the Gaussian portion of this model can be reduced to zero, all that will remain is the contributions of the continuum underneath the peak. In other words, if the value of *a(3)* can be minimized, the library is said to have been removed. Fortunately fitting a peak in a collected spectrum is relatively easy with today's solvers; unless otherwise noted all fits performed were accomplished by the

CURMOD program. The first step toward library removal, once a target library and corresponding peak in the unknown spectrum has been identified, is to determine the amount of the library to subtract. An obvious method would be to perform a fit with the model above and apply the *a(3)* constant across the target library and then subtracting that library from the unknown. The results of this operation on the spectrum shown in Figure 11 are shown below.

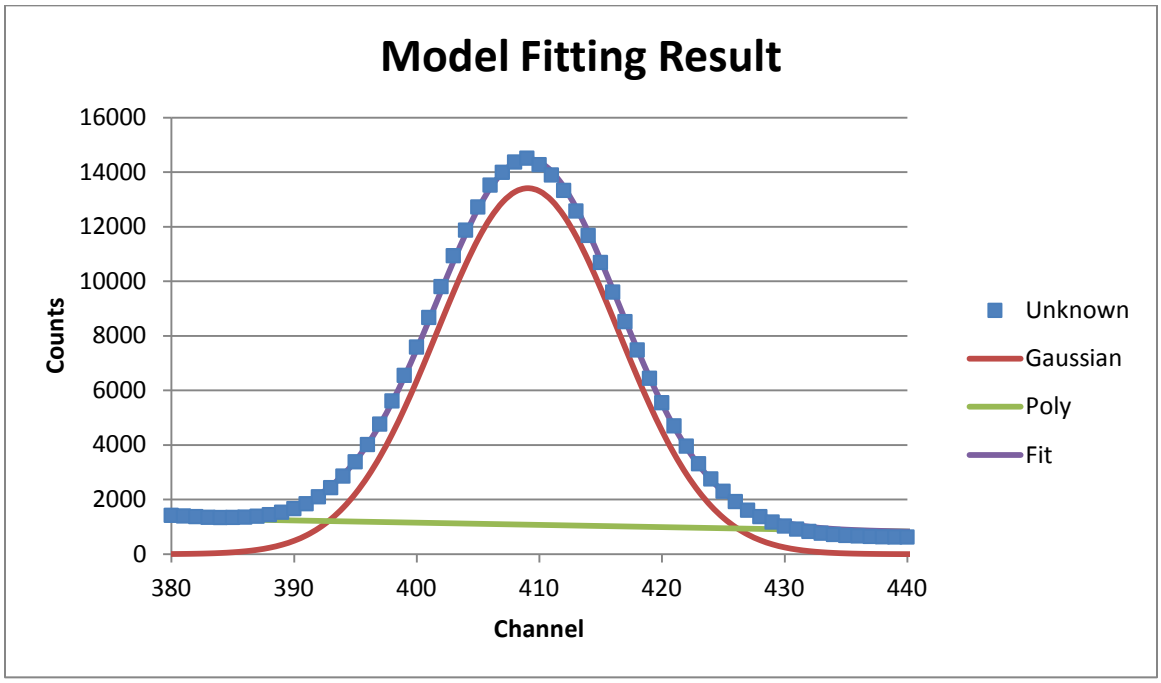

Figure 12: Fitting Model Plotted Against Peak of Interest

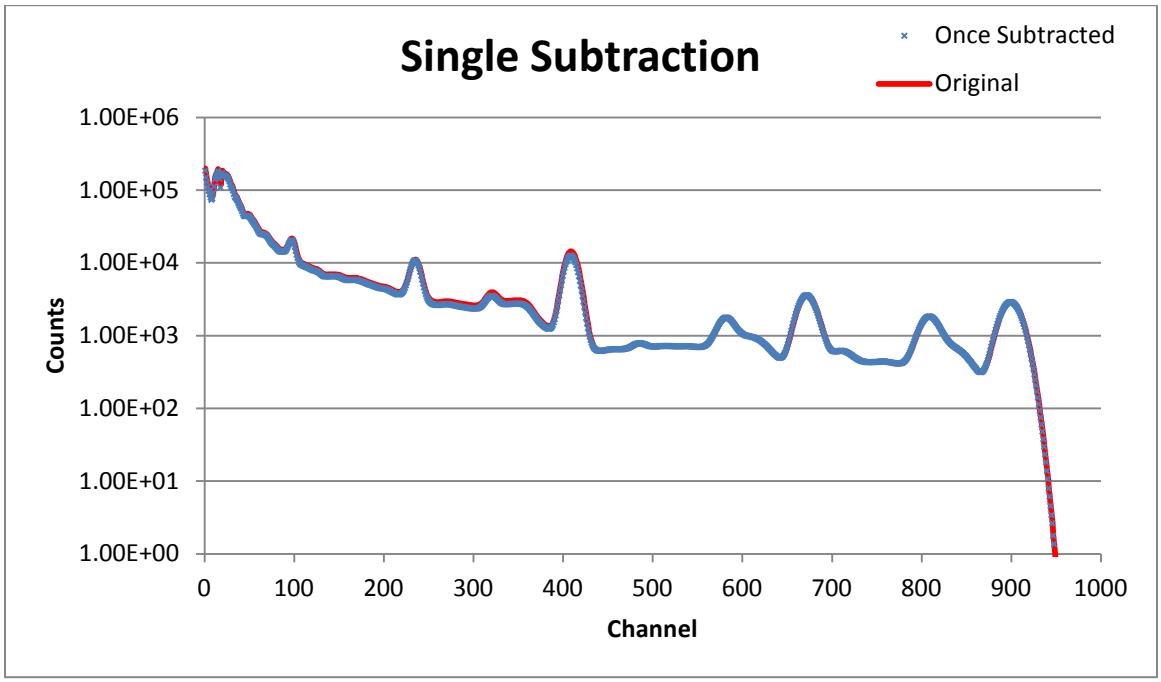

Figure 13: Result of Attaching a(3) to the H library and Subtracting from Spectrum

Table 4: Solved Fitting Parameters for Example Spectrum

A(1)	409.0795
A(2)	7.416952
A(3)	13411.89
A(4)	-8.15809
A(5)	4412.718
χ^2	1.1829

Figure 12 and Table 4 seem to indicate a very good fit of the model to the targeted peak. However, Figure 13 shows that the value for *a(3)* vastly underestimates the magnitude of the contribution of the hydrogen library to the spectrum. The reason for this is that the library spectrum describing hydrogen, and indeed every library spectrum, covers more than just the peak area. When a library is subtracted from the unknown spectrum the continuum on the

low energy side of the peak is altered as well as the peak itself. When the continuum changes, the model described in Equation 21 will no longer correctly describe the peak in question. In order to move forward with this idea of subtracting down to the continuum as a method for library removal an iterative method was adopted.

Iterative Subtraction

As a single round of subtraction was not enough to remove the contribution of a library using the method as described, a new procedure was developed. A peak in the unknown spectrum that corresponds to a library spectrum is identified, and the model described in Equation 21 is applied. The fitted constant *a(3)* is multiplied across the entire library spectrum, and the resulting spectrum is subtracted from the unknown spectrum. So far, the method has not changed from what was described in the previous section. However, the residual of this subtraction is now taken to be a new unknown spectrum, and the fitting model is applied across the same channel range as the first fit. A new *a(3)* constant will be generated and will be applied across the corresponding library for subtraction again. This process will continue until the polynomial portion of the model is the primary contributor to the fit across the channel range. An example of this process can be found in Figure 14 below, where the spectrum described in Figure 11 is being operated on.

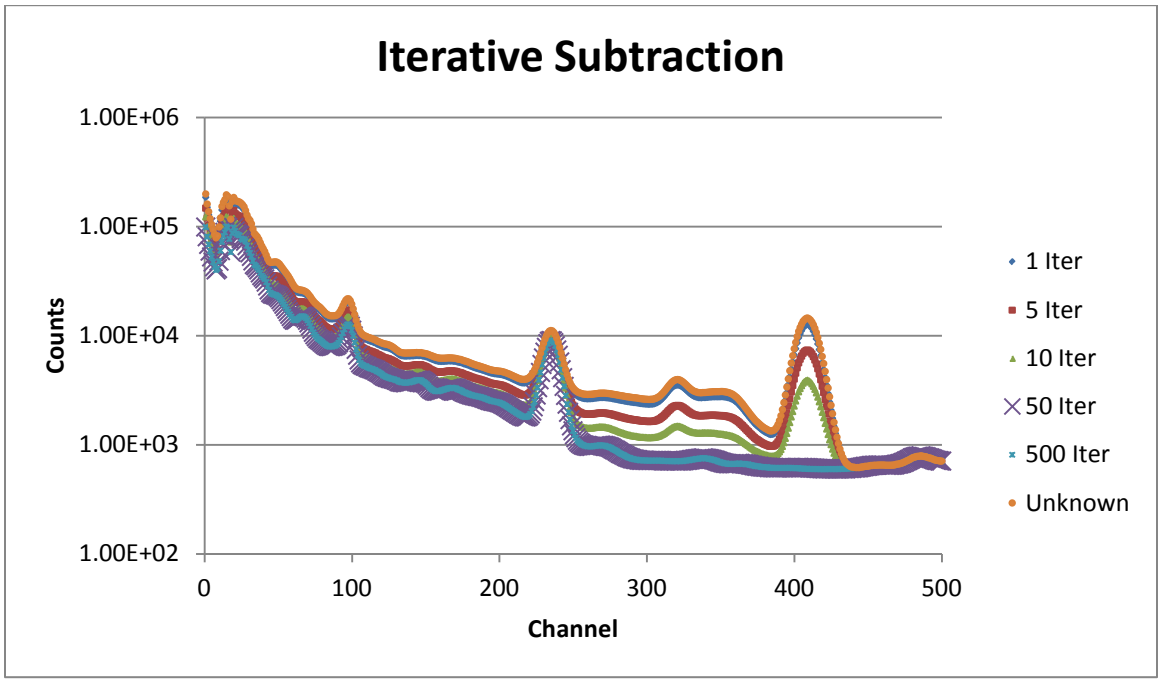

Figure 14: Iterative Subtraction of H Library

Clearly after several iterations the contribution of the hydrogen library has been removed while leaving the contribution of the carbon library intact. The convergence behavior of this method can be found in Figure 15, where the data points describe the cumulative library multiplier attached to the hydrogen library in the fit above. There appears to be a point at which the multiplier attached to the Gaussian portion of the fitting model no longer contributes to the fit across the peak channel range, as evidenced by the plateau visible in Figure 15.

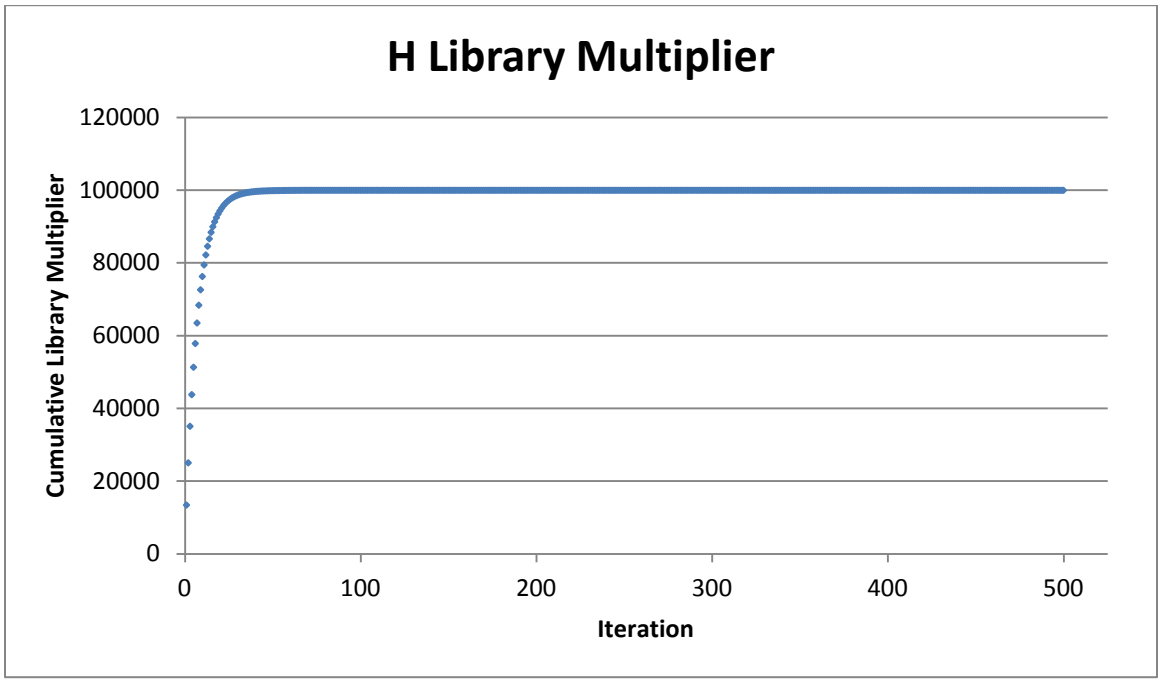

Figure 15: Convergence Behavior

When this plateau is reached, the process is said to have converged and the loop exits.

Convergence Dampening

The example spectrum in Figure 11 is a very best case scenario for the application of this method. There is no statistical noise, there are few radioisotopes involved, and the radioisotope libraries used for subtraction perfectly describe the radioisotope's contribution to the unknown spectrum. These conditions cannot be achieved in realistic testing conditions, and realistic testing conditions bring additional challenges to applying this method of subtraction. A possible effect of less than ideal conditions can be shown in the figures found below.

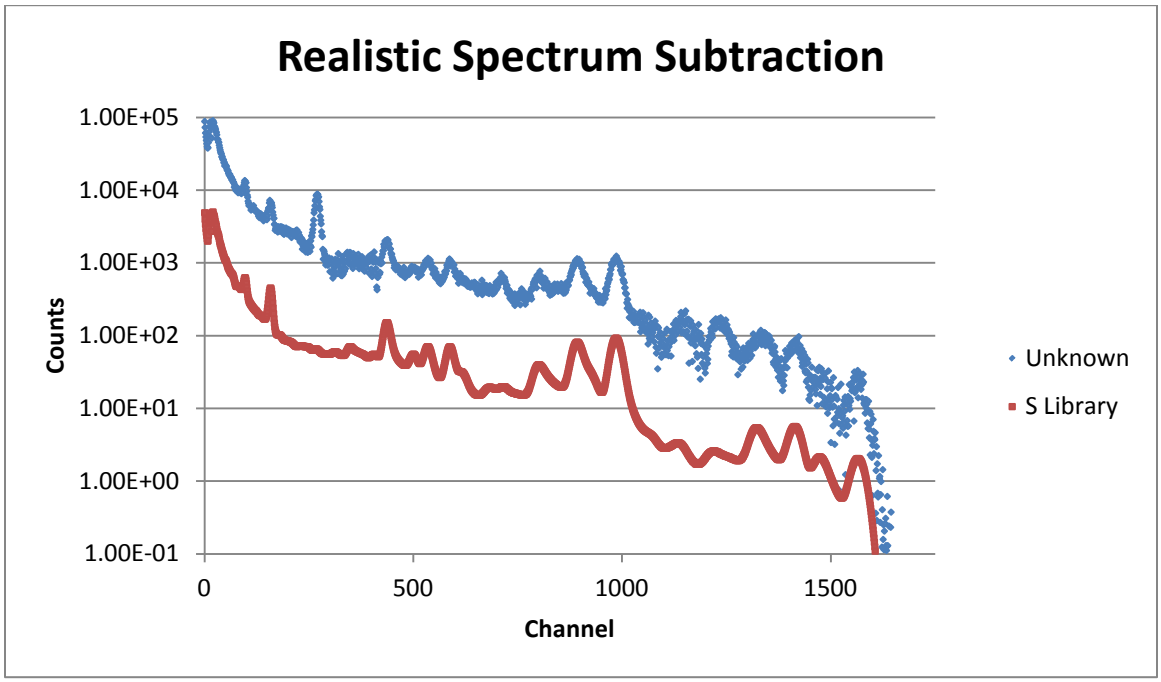

Figure 16: Realistic Spectrum Example

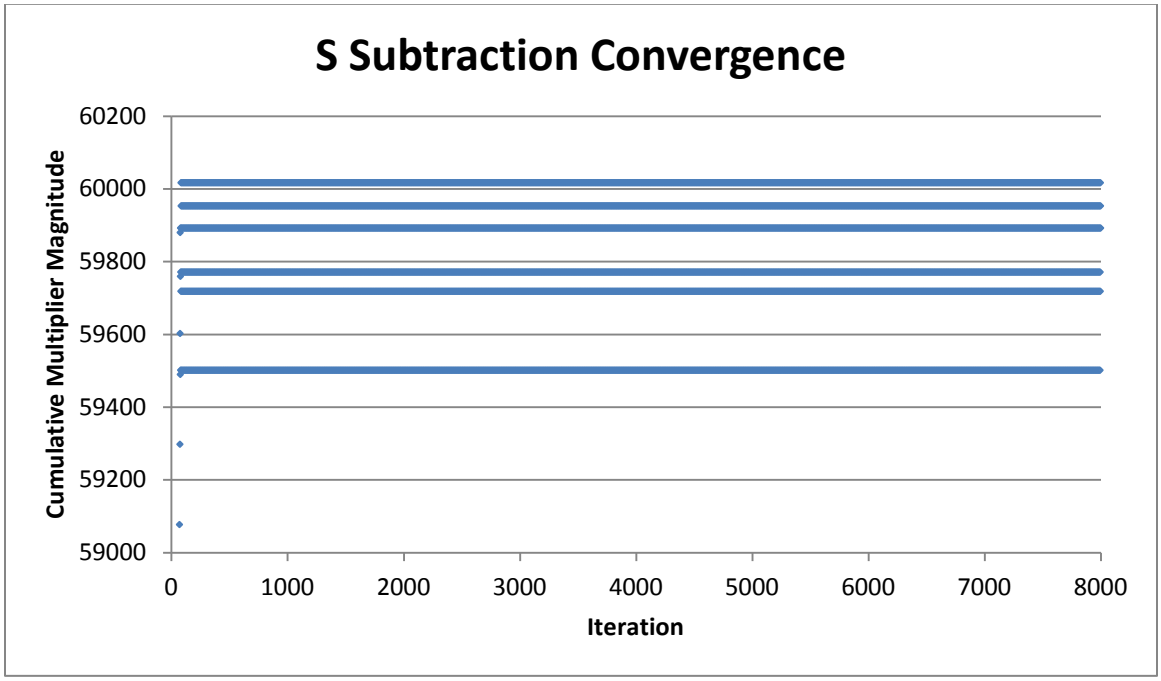

Figure 17: Realistic Spectrum Subtraction Convergence

Figure 17 shows that the process is not converging. The magnitude of the Gaussian model is fluctuating between a positive and negative value without a decrease in magnitude. The final value is then just determined by the value at the final iteration, which is not acceptable. In order to combat this, a gradually decreasing dampening constant is introduced. The dampening constant is applied to the Gaussian magnitude before it is applied to the library for subtraction, with the goal of lessening the magnitude of the fluctuations of the cumulative multiplier. This will, given enough iteration, hopefully allow for the convergence of the process in situations where convergence would otherwise not be possible. This damping constant is applied in stages as to preserve the initial behavior of the undamped subtraction process while forcing eventual convergence. This implementation can be found in Table 5 and Figure 18 below.

Table 5: Dampening Constant Application Scheme

Iteration Number	Dampening Constant
0-1999	1
2000-4999	0.5
5000-5999	0.1
6000-6999	0.05
7000-8000	0.01

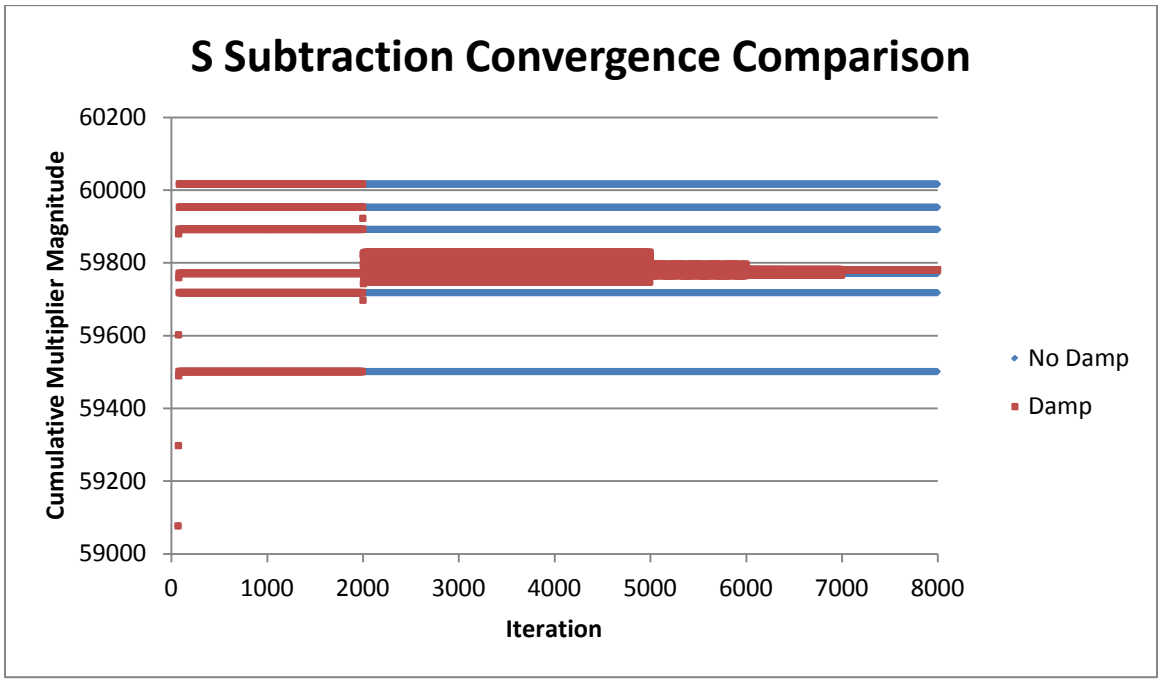

Figure 18: Damped vs. Undamped Convergence Comparison

This figure shows that by applying a dampening constant in this way a converged solution can be found where there would otherwise be none.

Count Threshold after Subtraction

After all known libraries have been subtracted, it is likely that a band of noise will remain above any peaks uncovered in the course of applying the method. This band of noise is the result of differing counting statistics between the library and the unknown spectrum. It is very likely that the unknown spectrum will have more counts in the areas that a subtracting library covers; the different amount of counts will result in a different amount of relative spread between the two data sets. To combat this, a threshold method has been adopted to determine where statistically significant features begin in the final residual spectrum.

Essentially a threshold value is determined and compared against the number of counts in a channel. If the threshold value is greater than the number of counts in that channel, the number of counts in that channel is said to be not significant and is set to zero. If the number of counts is greater than the threshold value, the number of counts is significant and is left alone. This procedure is applied to all channels in the residual spectrum. The threshold value is determined by Equation 22, where *yi* is the number of counts in channel *i* and *imax* is the maximum number of channels.

Equation 22: Threshold Value Determination

$$Threshold = \sqrt{\frac{\sum_{i=i}^{imax} y_i}{imax}}$$

Convolved Peak Subtraction

A situation may arise where the highest intensity peak of one library is convolved with a peak of another library. Applying the subtraction method as described so far will lead to inaccurate results to a convolved peak, but that does not mean that convolution completely excludes such a peak from consideration. Instead the fitting model can be modified to fit the new situation and the subtraction of the convolved library can proceed simultaneously. As both peaks will be on top of the same continuum, the only change needed to the model described in Equation 21 is the addition of another Gaussian function to accommodate the second library peak. The convolved peak fitting function can be found below in Equation 23.

Equation 23: Convolved Peak Fitting Model

$$Gaussian1 = a(5) * \exp\left(-\frac{\left(\mathrm{x} - \mathrm{a}(1)\right)^2}{2 * \mathrm{a}(2)^2}\right)$$

$$Gaussian2 = a(6) * \exp\left(-\frac{\left(\mathrm{x} - \mathrm{a}(3)\right)^2}{2 * \mathrm{a}(4)^2}\right)$$

$$Polynomial = a(7) * x + a(8)$$

$$Model = Gaussian1 + Gaussian2 + Polynomial$$

This model would be applied across the specified channel range of a convolved peak in the unknown spectrum, yielding Gaussian multipliers *a(5)* and *a(6)*. These multipliers would then be applied to the corresponding libraries and subtracted from the unknown spectrum. The subtraction would then iterate until only the polynomial had a significant contribution to the fit; at that point, both libraries involved are said to have been removed. In practice, however, it was found that CURMOD often struggled to resolve the four nonlinear parameters involved in this model. This is most like because the peak center (*a(1)* and *a(3)*) as well as the standard deviations (*a(2)* and *a(4)*) are very similar to each other. After all, since they are convolved, the centers of the two peaks must be close together, and since they occupy a very similar energy range the width of the peaks will be similar as well. To simplify the fit and allow the solver to work with a more linear model a modified procedure was adopted. The single peak fitting model was applied to both libraries before the subtraction process began. The peak center as well as the standard deviation in the Gaussian model was extracted for both of the library peaks. These values were set as constants in the convolved peak model shown above, replacing variables *a(1)* through *a(4)*. With the nonlinear parameters of the Gaussian functions fixed the iterative subtraction is now wholly linear, which improved the stability of the process significantly. A variable dampening

scheme was applied to both of the produced library multipliers; this was done in the same form and for the same function as in the single peak subtraction method.

Artificial Spectra Creation

In order to benchmark these methods, an "unknown" spectrum with known contributions from established libraries was desired. This would allow for a comparison between the known magnitude of the library versus the solved magnitude of the library after the subtraction method was completed. In order to do this five neutron activated prompt gamma libraries and one natural background library were obtained from the code CEARCPG (Han, 2007). The prompt gamma ray libraries were hydrogen (H), calcium (Ca), carbon (C), sulfur (S), and phosphorus (P). The natural background library was potassium-40 (k40). These libraries can be found in Figure 19 below.

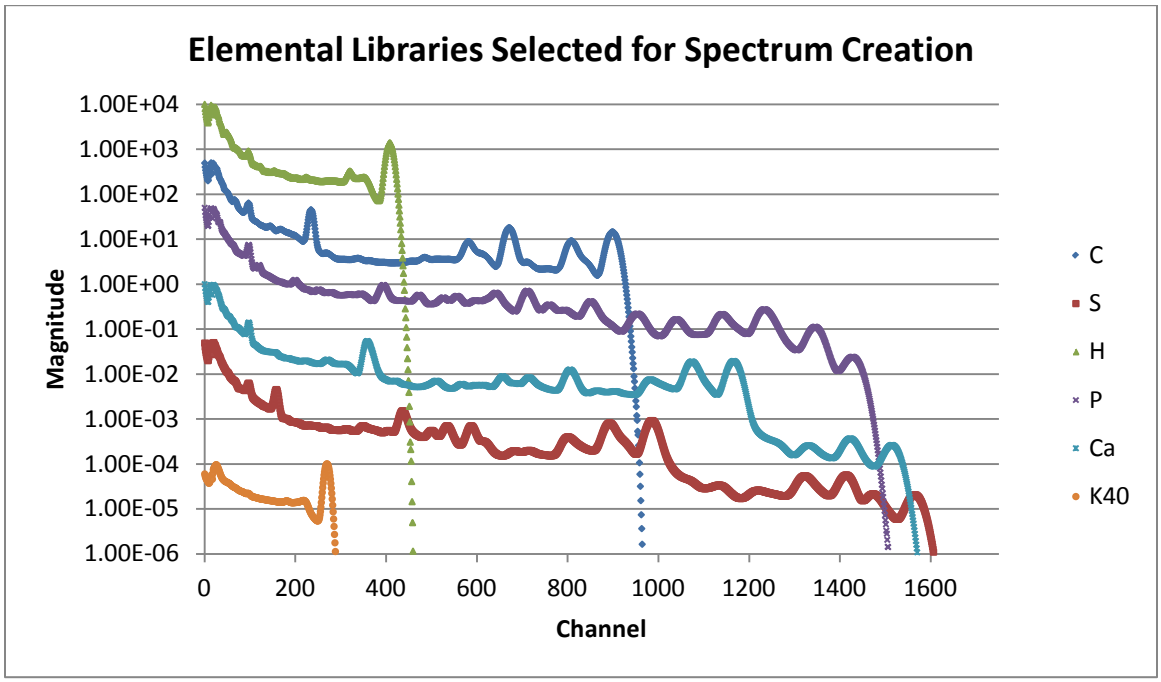

Figure 19: Prompt Gamma and Background Libraries included in Artificial Spectra

These libraries were chosen simply because they feature a wide range of peaks across a large number of channels. A combination of these libraries is not meant to approximate a specific real world scenario; the purpose is to test the subtraction method on a spectrum that is relatively complex. The first step for creating an artificial "unknown" spectrum is to sum these libraries together across all channels. The values in Table 6 are applied to their respective libraries after each library is normalized to their highest value. The magnitudes found in this table again come from Xiaogang's work on the CEARCPG code (Han, 2007). They were chosen simply to have a range of contribution among the included libraries rather than having equal multipliers. Figure 20 shows the summation of these libraries after they have been multiplied.

Table 6: Library Multipliers

Library	Multiplier
C	32030.5
S	60717.3
H	627374
P	23108.6
Ca	25226.3
K40	10650.5

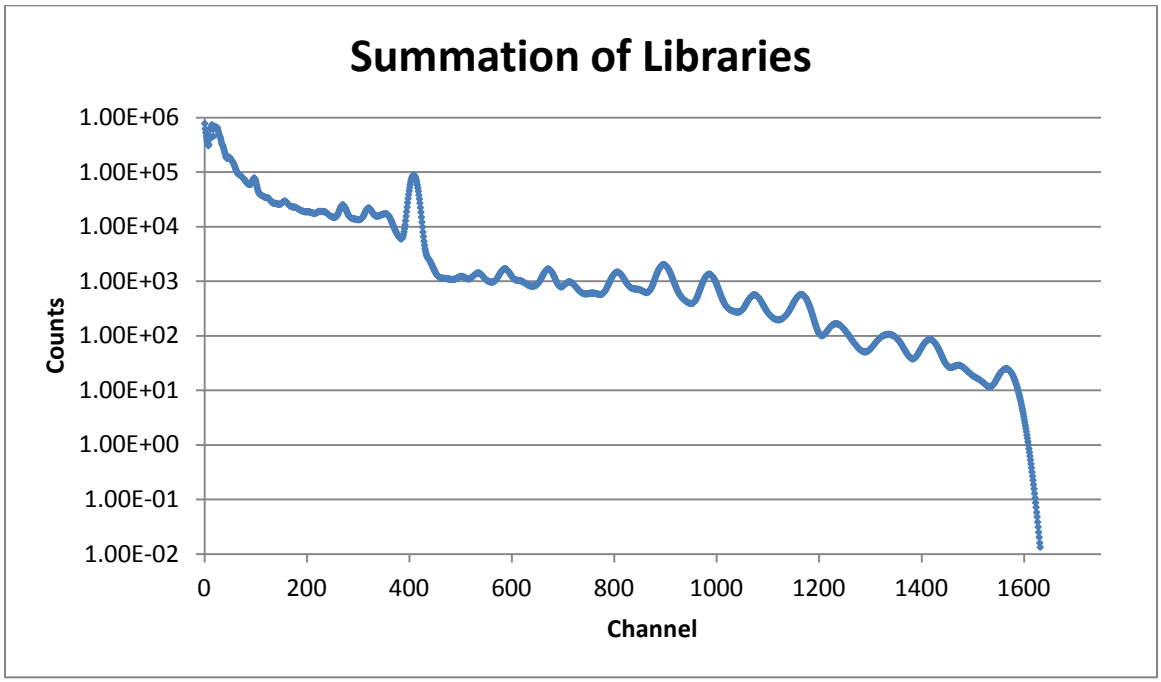

Figure 20: Summation of Chosen Libraries

This spectrum could be used for testing, but it neglects the affect counting statistics have on a collected spectrum. In order to add an element of counting statistics to this spectrum, the number of counts in each channel is scattered by a Gaussian random number. This number is generated by performing a Box-Muller (Box, 1958) transformation on a uniform random

number, as uniform random numbers are easy to generate in FORTRAN. This transformation takes the form shown in Equation 24, where x_1 and x_2 are uniformly distributed random numbers between zero and one and y_1 and y_2 are Gaussian distributed random numbers with zero mean and a standard deviation of one.

Equation 24: Box-Muller Transformation

$$y_1 = \sqrt{-2 \ln x_1} \cos 2\pi x_2$$

$$y_2 = \sqrt{-2 \ln x_1} \sin 2\pi x_2$$

To apply these Gaussian random numbers to the counts in a channel the following equation is used:

Equation 25: Application of Gaussian random numbers to spectrum

$$G = C + y * \sqrt{C}$$

Where C is the original count in the channel, y is a Gaussian distributed random number, and G is the Gaussian distributed count for that channel. Figure 21 shows the application of this process across the entire unknown spectrum.

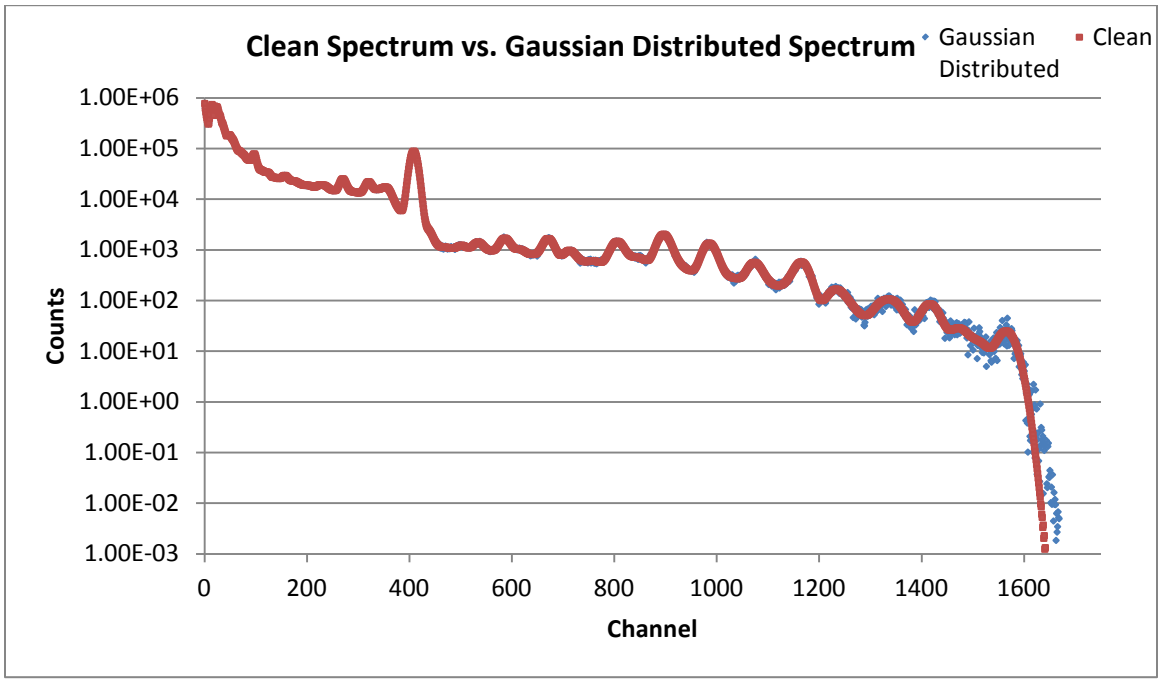

Figure 21: Gaussian Distributed Spectrum compared to Clean spectrum

As would be expected in a real spectrum, the counting statistics grow noticeably worse as the number of counts go down. This spectrum will be an idea test case to prove the subtraction method laid out in the previous sections has merit. The unknown spectra created in the following sections will all be created in this manner.

Application of Iterative Subtraction Method to Artificial Unknown Spectra

To demonstrate the proposed iterative subtraction method, two separate artificial spectra have been created. These spectra contain six pre-generated libraries, namely H, Ca, C, S, P, and K40. K40 will act as a background source of radiation present in the unknown spectrum that

the operator's collection of library spectra do not cover. The known libraries H, Ca, C, S, and P will subtracted out of the unknown spectrum in that order and the final residual will be compared to the missing library K40 as a metric of success. A library least-squares fit of the unknown spectrum both with and without the calculated background spectrum will be performed, with the accuracy of the library magnitudes being the second metric for the success of the subtraction method. The two artificial spectra differ in the magnitude of the K40 background library; in essence, one spectrum will represent a case where a background source is a significant contributor to the total number of counts and the other will represent a case where a missing source of background contributes relatively few counts.

High Background Artificial Spectrum Analyzed by Iterative Single Peak Subtraction

The unknown spectrum created for this analysis can be found in Figure 22; the library magnitudes used to create this spectrum can be found in Table 7. Figure 23 through Figure 27 show the results of the subtraction method. The subtraction was done in the order presented by these figures. Each of these figures will present data in the following way: the topmost graph will show the spectrum that will be operated on and the library that will be subtracted, the middle graph will show the convergence behavior of the iterative subtraction, and the bottom table will show the chi-squared value describing the model fit at the final multiplier across the channel range shown as SubStart/End, the final library multiplier the subtraction process converged to, and the percent difference of this final multiplier to the corresponding true multiplier found in Table 7. Figure 28 will show the metrics for the

success of the subtraction. The top third will show the application of the threshold as determined by Equation 22. All values below the value indicated in this section of the figure will be zeroed. The middle third of this figure will show the fit of the actual missing library, K40, to the final calculated missing library after the threshold has been applied. The chi-squared value for this fit will be displayed on this section of the figure. The lower third of this figure will show the results of a library least-squares fit of the unknown spectrum in Figure 22 with two different sets of libraries. The first fit will be performed only with the libraries C, S, H, P, and Ca. The second fit will use these same libraries as well as the calculated background library shown in the top half of this figure. The solved multipliers for both of these library least-squares fits as well as a percent difference to the corresponding values in Table 7 will be shown.

Table 7: High Background Artificial Spectrum Library Multipliers

Library	Multiplier
C	32030.5
S	60717.3
H	627374
P	23108.6
Ca	25226.3
K40	128076

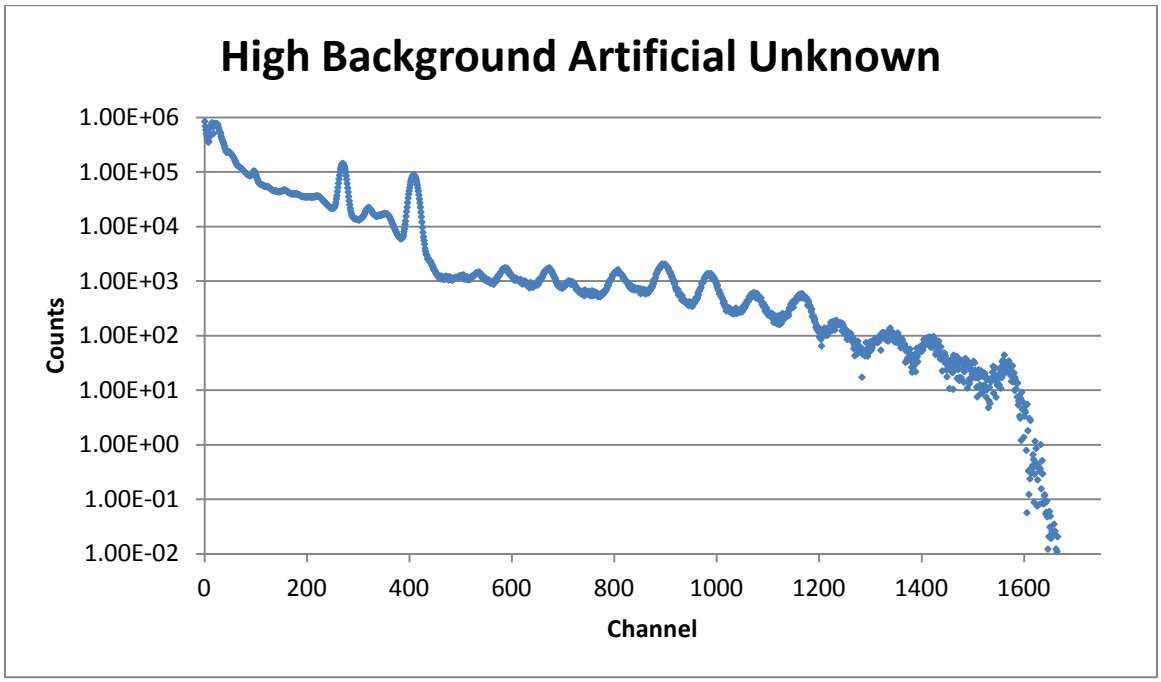

Figure 22: High Background Unknown

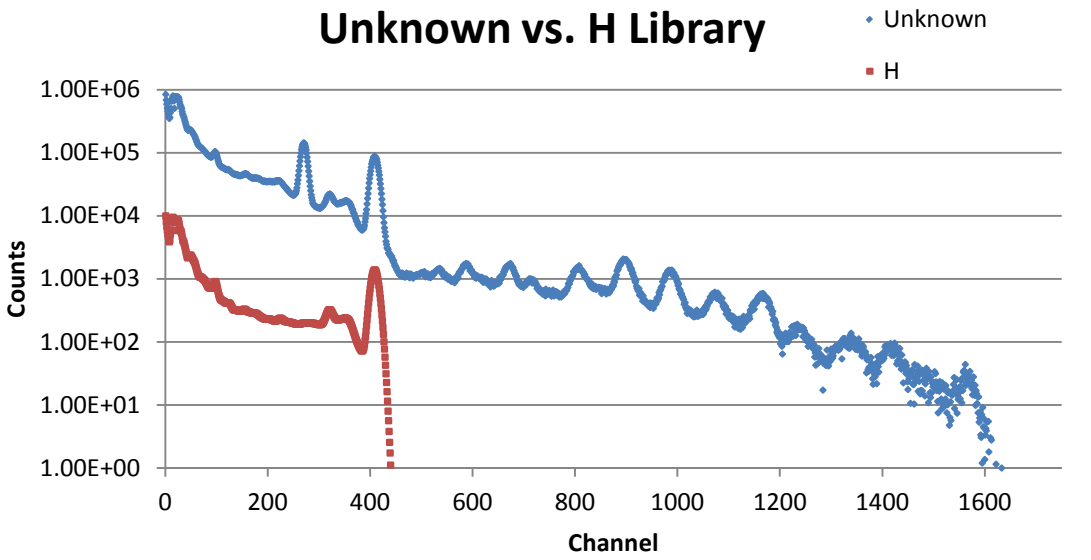

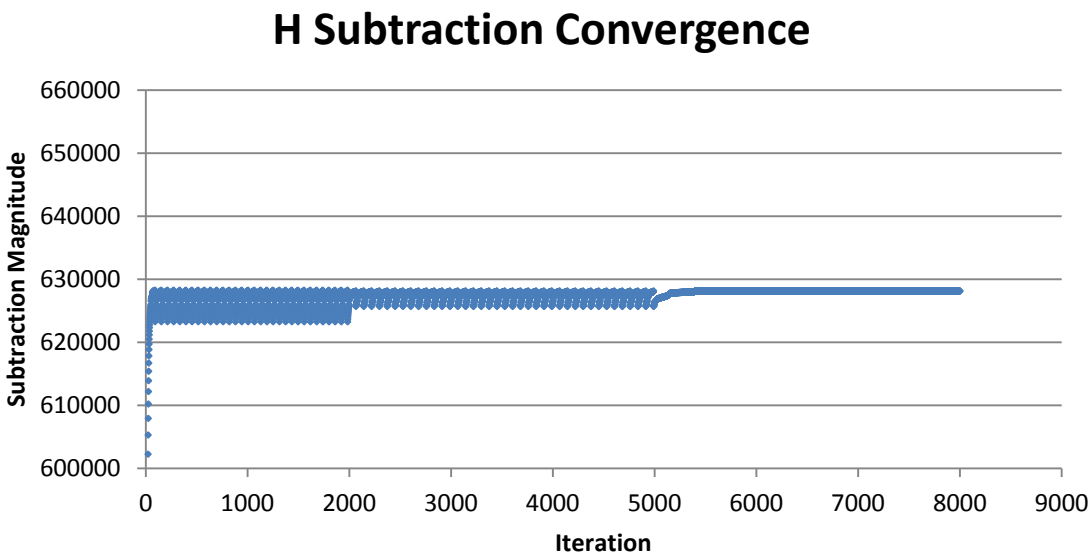

Chisquared	146.8367
SubStart/End	380,425
Multiplier	628179.6993
% Difference	0.12842408

Figure 23: High Background H Subtraction

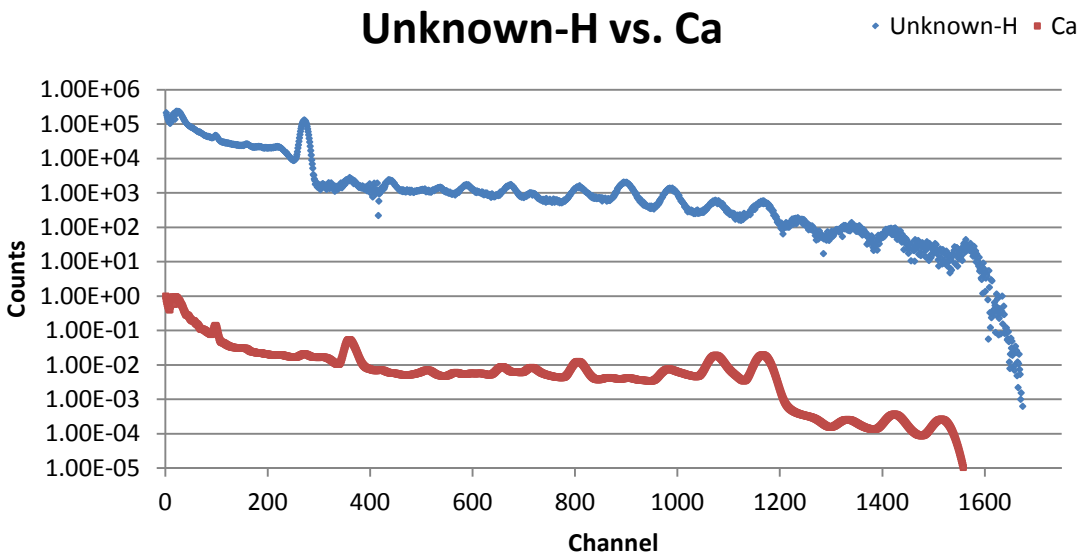

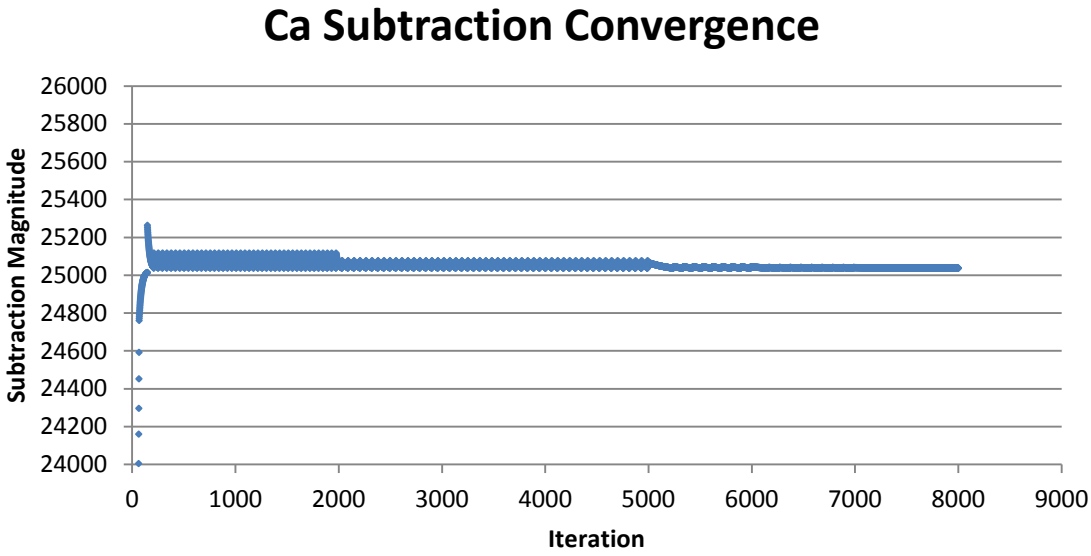

Chisquared	23.7826
SubStart/End	335,384
Multiplier	25042.06434
% Difference	0.73033168

Figure 24: High Background Ca Subtraction

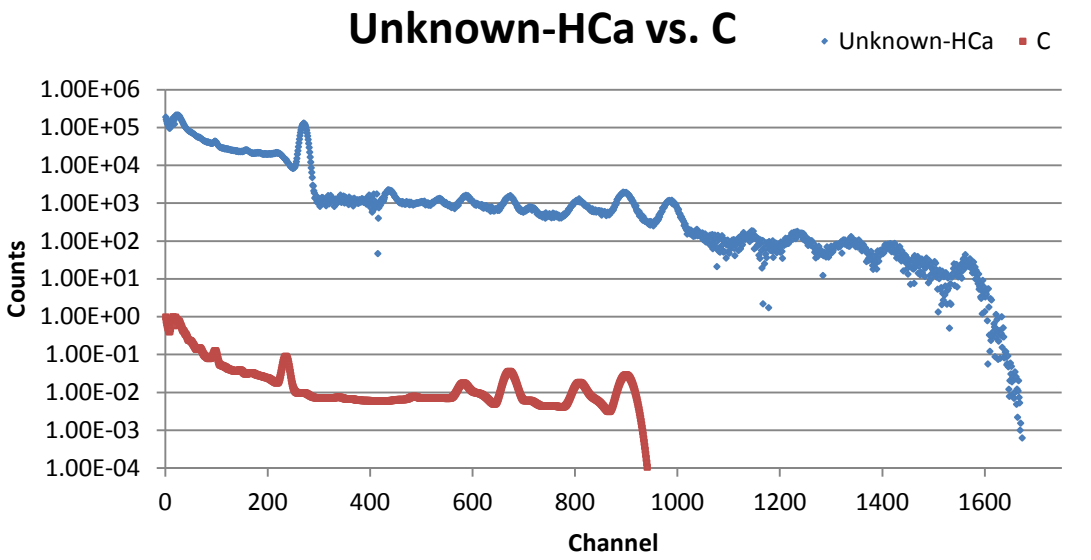

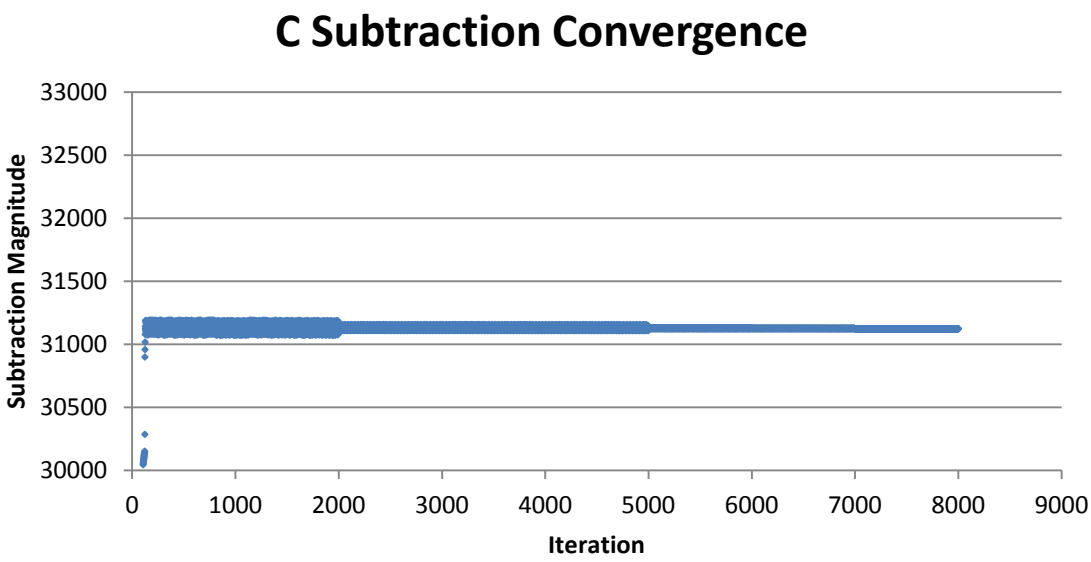

Chisquared	5.7639
SubStart/End	649,690
Multiplier	31125.1014
% Difference	2.826676437

Figure 25: High Background C Subtraction

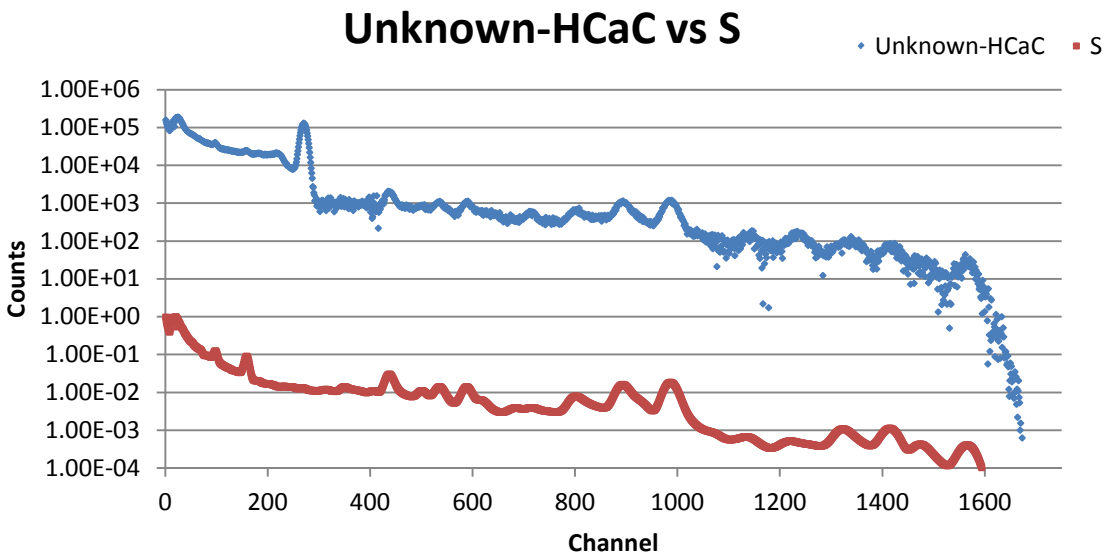

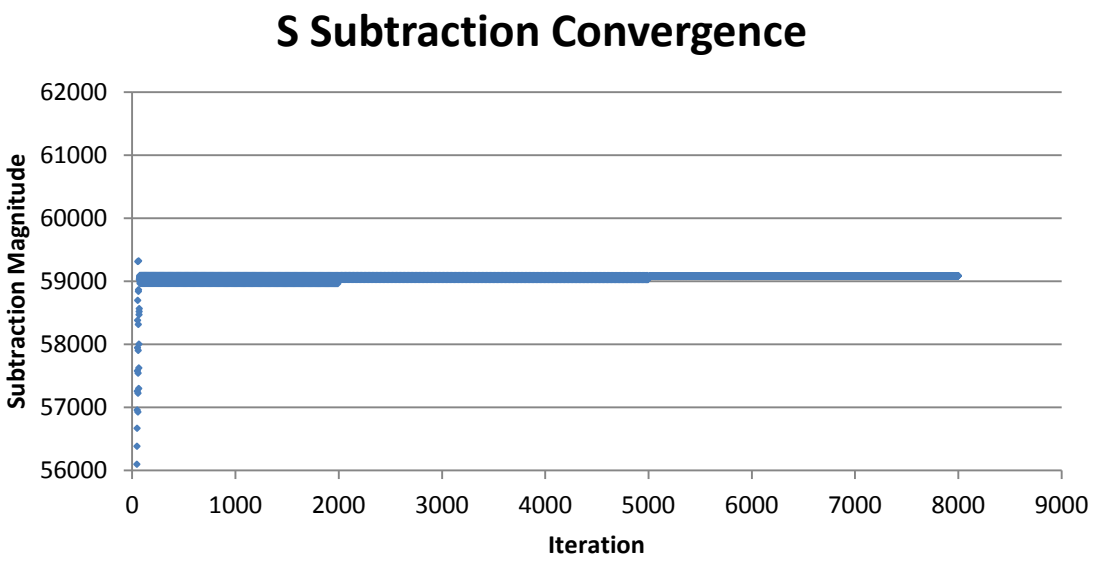

Chisquared	3.9917
SubStart/End	143,170
Multiplier	59091.34827
% Difference	2.677905189

Figure 26: High Background S Subtraction

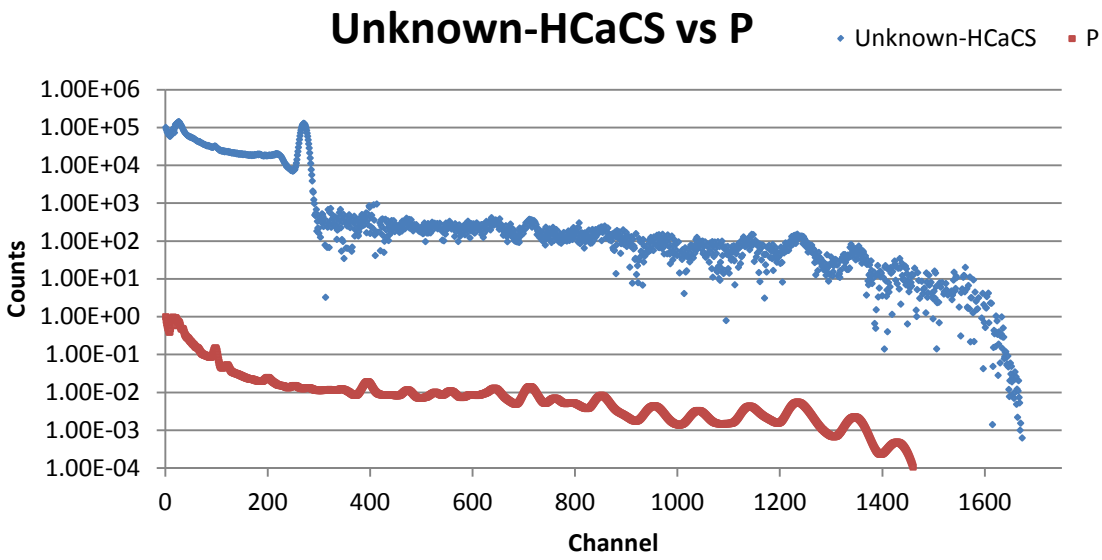

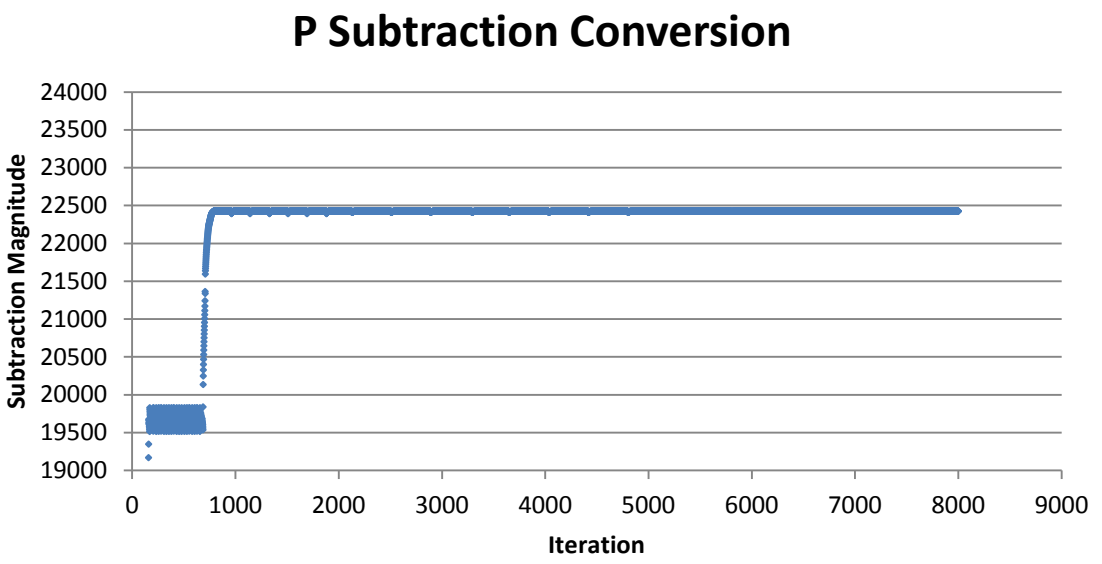

Chisquared	36.857
SubStart/End	690,730
Multiplier	22427.6568
% Difference	2.946709029

Figure 27: High Background P Subtraction

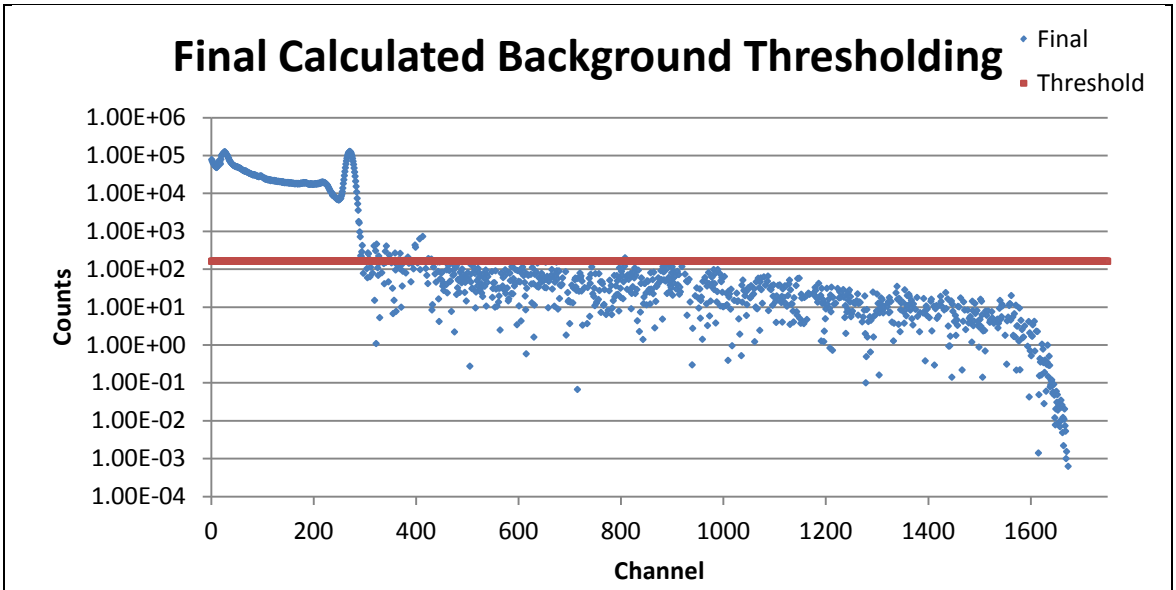

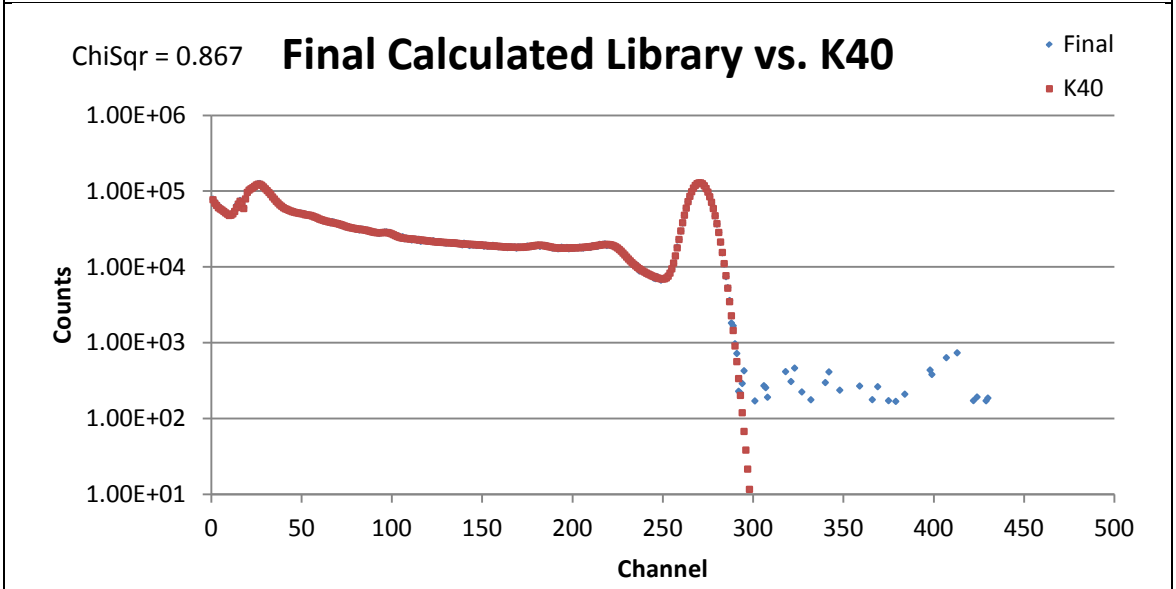

Library	LLS Multiplier w/o Bkgd	LLS Multiplier with Bkgd	% Difference w/o Bkgd	% Difference with Bkgd
H	793465	626779	26.47400115	0.094839761
Ca	22868.7	25078.2	9.345801802	0.5870857
C	40349	32643.7	25.97055931	1.914425313
S	59957.7	60015.4	1.251043772	1.156013196
P	23283.9	22942.9	0.758592039	0.717049064

Figure 28: High Background Final Calculated Library Comparison to True Background Library

Convolved Peak Subtraction Method Applied to High Background Artificial Spectrum

To demonstrate the convolved peak subtraction method on the unknown spectrum shown in Figure 22 a suitable convolved peak needs to be located. Such a peak exists in the unknown between the carbon and sulfur libraries. As the previous section demonstrated, single peaks suitable for subtraction can be found in this unknown spectrum, but for the sake of testing the subtraction of convolved libraries the subtraction of carbon and sulfur will occur at the same time. Hydrogen and calcium will be subtracted out using the single peak method the same way as in Figure 23 and Figure 24. The residual from that subtraction was used in Figure 29 below, and the phosphorus library was subtracted out via the single peak method as in Figure 27 above. After phosphorus was removed, the resulting residual spectrum was compared to the true missing library, K40, in the same way as in Figure 28. Both Figure 29 and Figure 30 are laid out as described in the previous section.

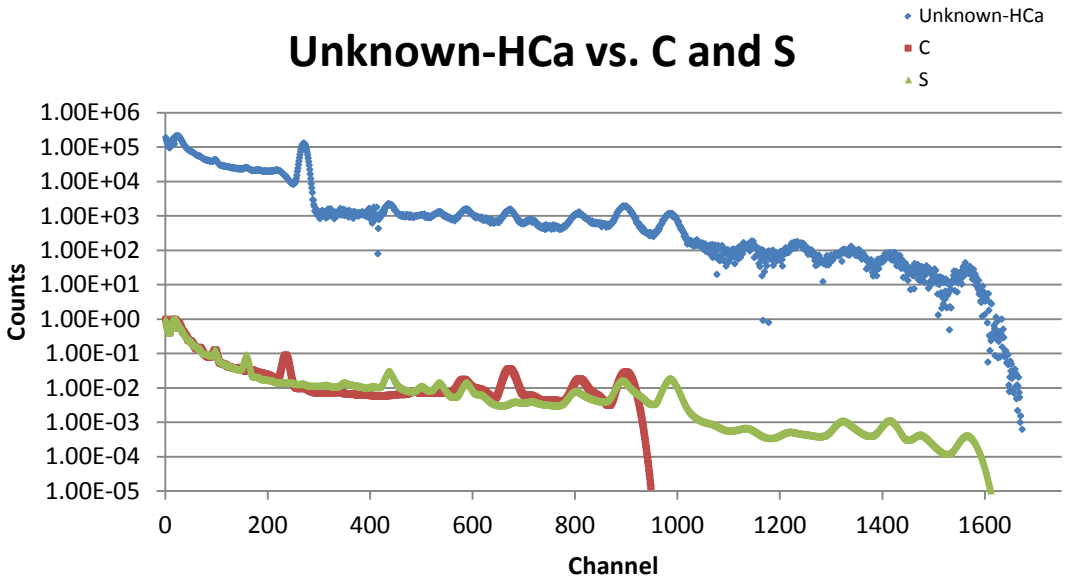

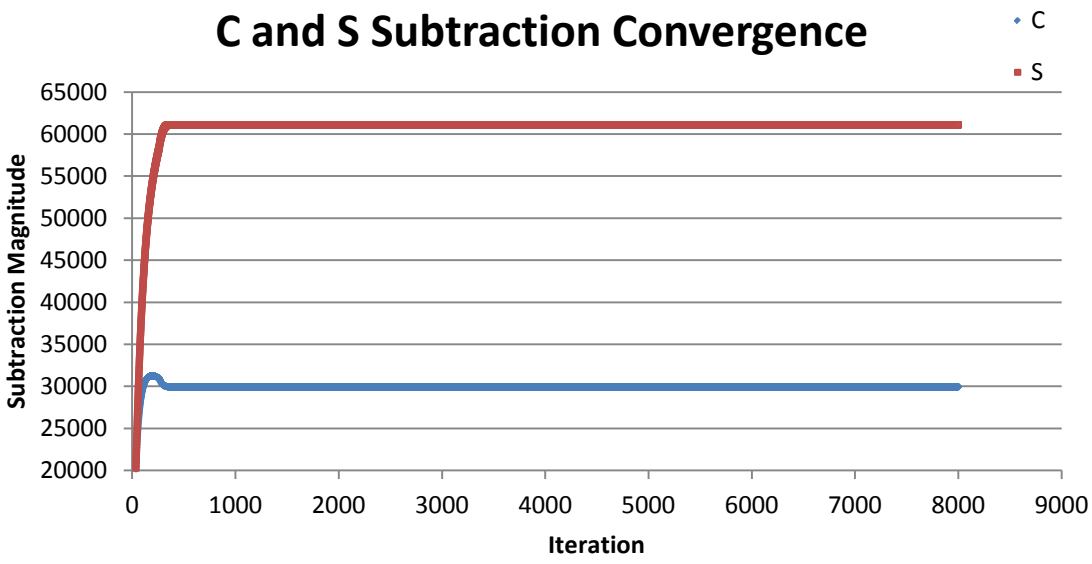

Chisquared	72.1263
SubStart/End	861,932
C Multiplier	29965.79
S Multiplier	61109.78
C % Difference	6.446075
S % Difference	0.646398

Figure 29: High Background C and S Convolved Subtraction

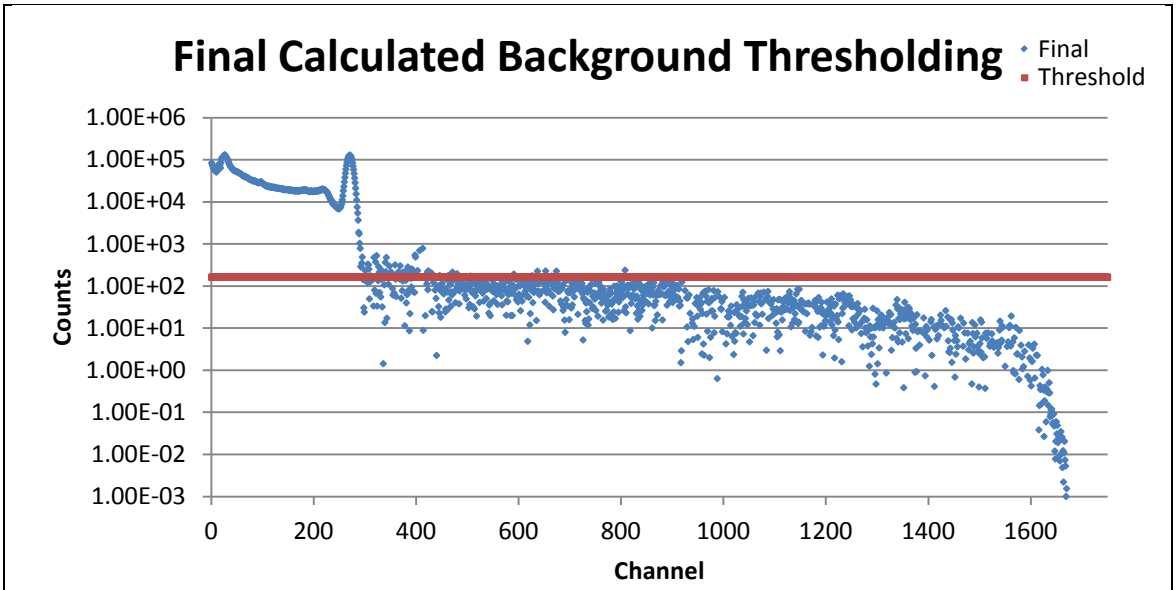

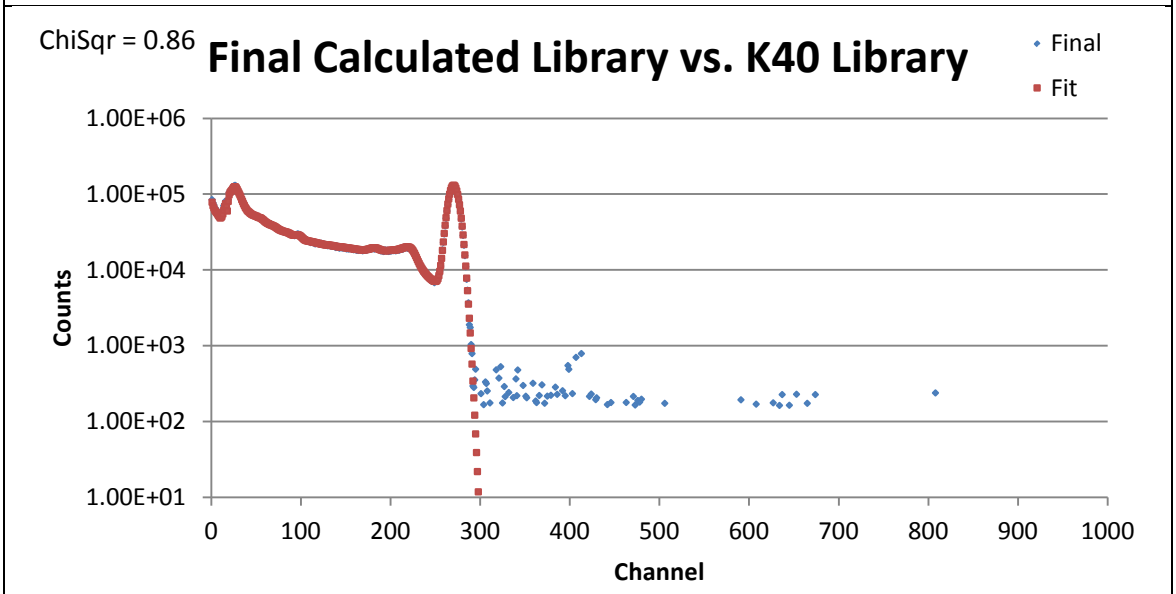

Library	LLS Multiplier w/o Bkgd	LLS Multiplier with Bkgd	% Difference w/o Bkgd	% Difference with Bkgd
H	793465	626779	26.47400115	0.094839761
Ca	22868.7	25078.2	9.345801802	0.5870857
C	40349	32643.7	25.97055931	1.914425313
S	59957.7	60015.4	1.251043772	1.156013196
P	23283.9	22942.9	0.758592039	0.717049064

Figure 30: High Background Final Calculated Library Comparison to True Background Library, Convolved Subtraction

Low Background Artificial Spectrum Analyzed by Iterative Single Peak Subtraction

The single peak subtraction detailed in the previous section will be performed on the unknown shown in Figure 31 constructed with the library multipliers shown in Table 8 below.

Table 8: Low Background Artificial Spectrum Library Multipliers

Library	Multiplier
C	32030.5
S	60717.3
H	627374
P	23108.6
Ca	25226.3
K40	7608

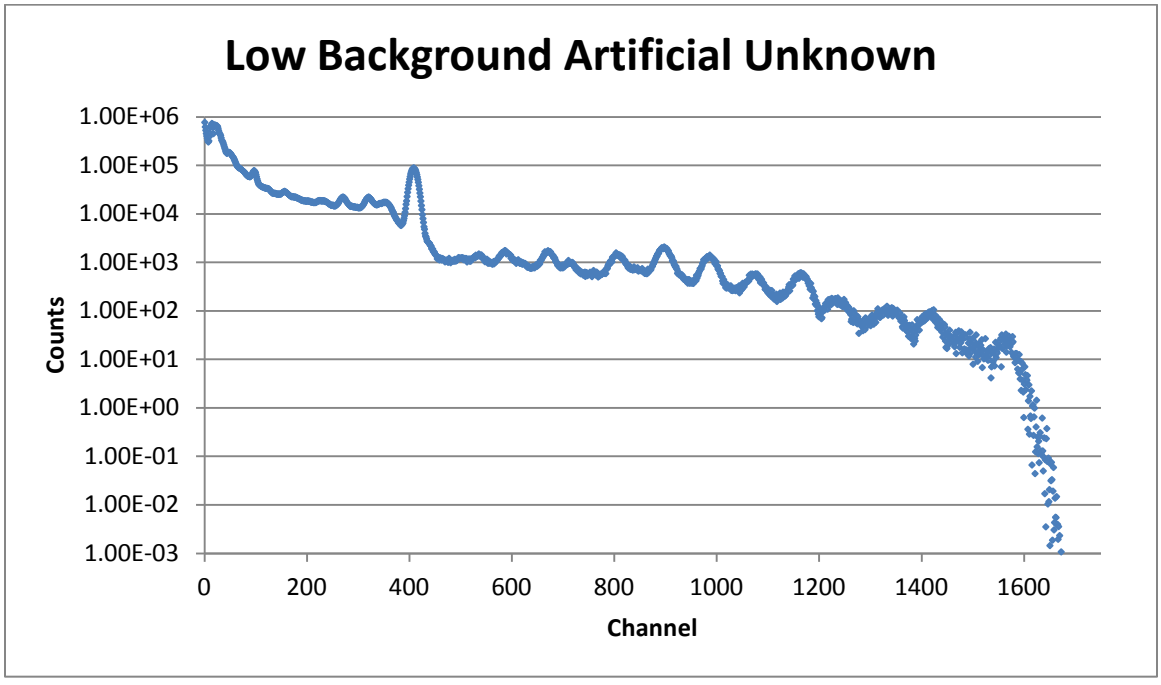

Figure 31: Low background Unknown

This spectrum will be subjected to the single peak subtraction method in the same way, by the same libraries, and in the same order as in the previous sections. The results of each library subtraction as well as the comparison to the true missing library will be presented in the same way as in the previous section as well.

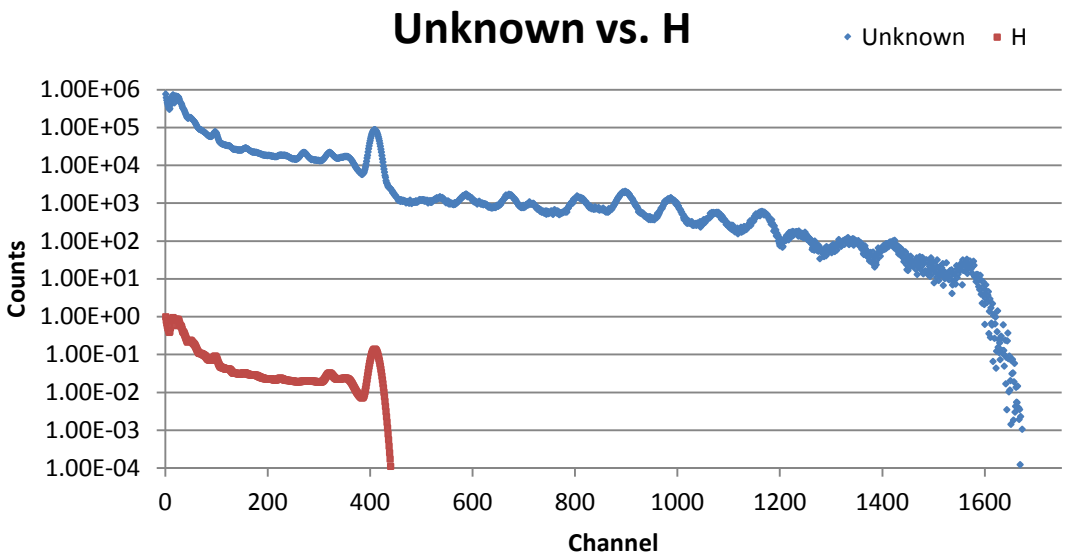

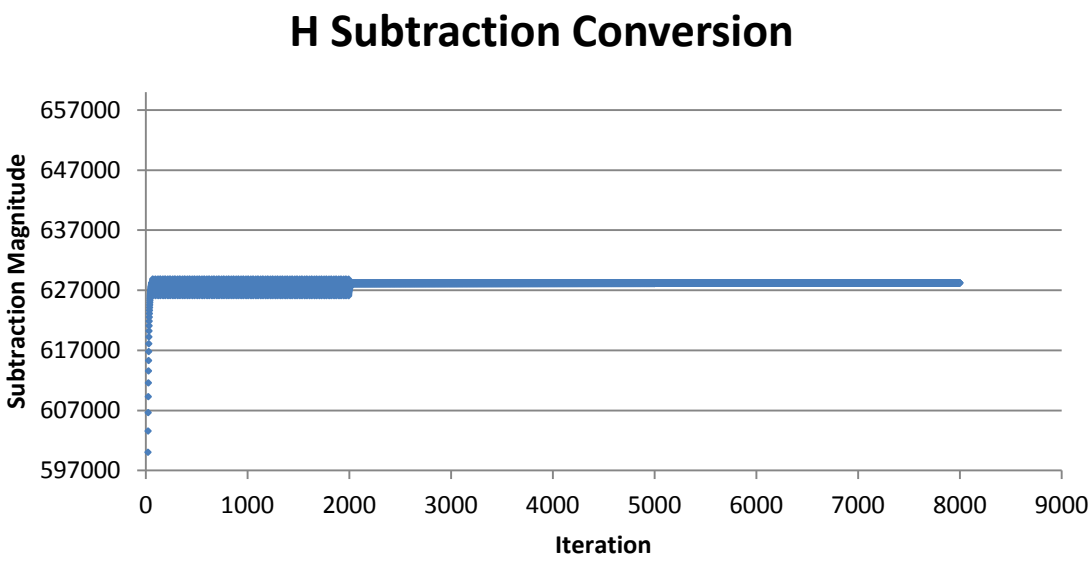

Chisquared	39.9984
SubStart/End	380,425
Multiplier	628198.7634
% Difference	0.131462803

Figure 32: Low Background H Subtraction

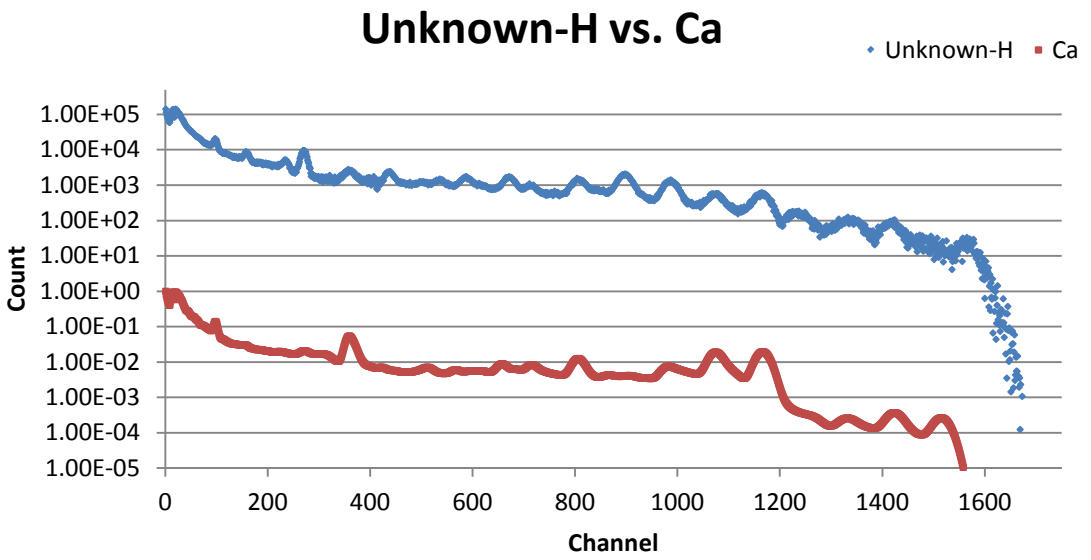

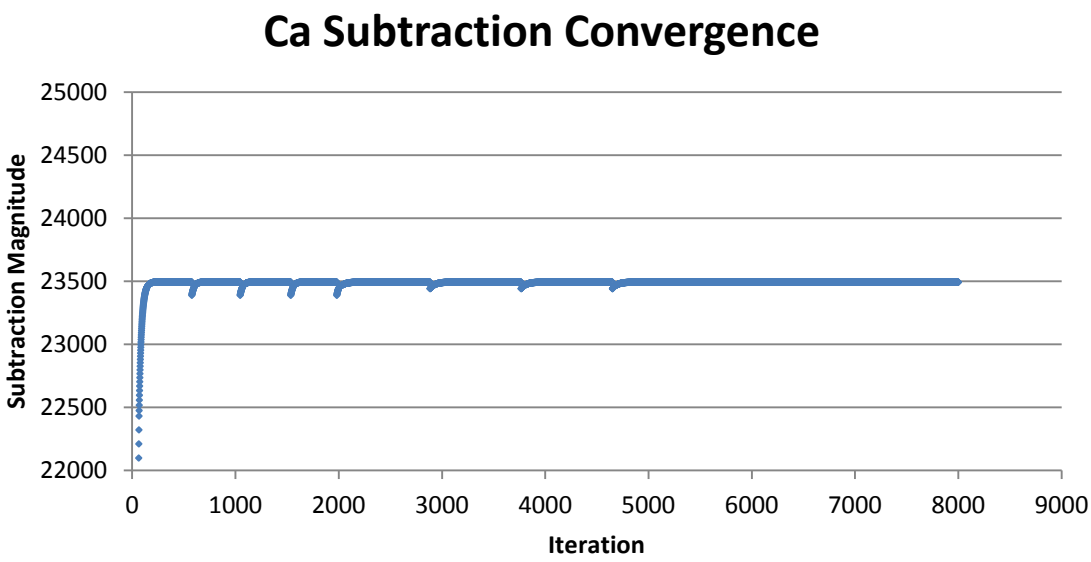

Chisquared	19.8109
SubStart/End	340,380
Multiplier	23494.75876
% Difference	6.864031739

Figure 33: Low Background Ca Subtraction

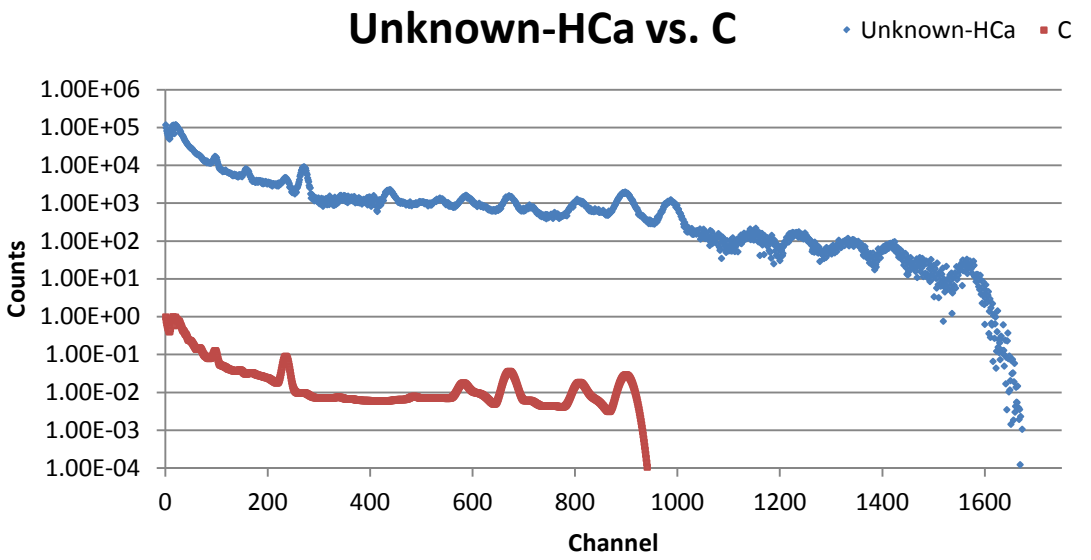

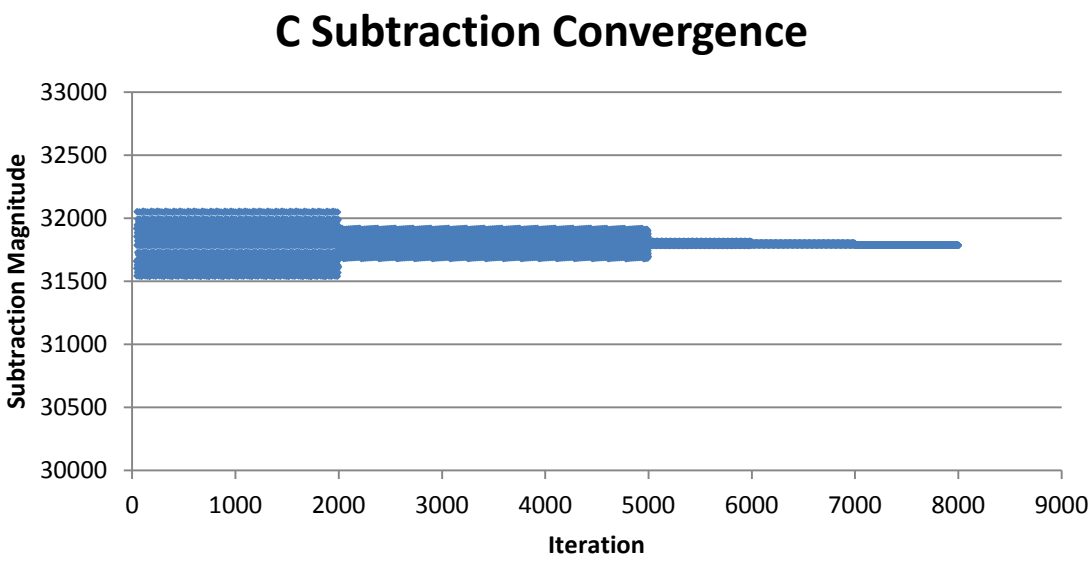

Chisquared	21.3472
SubStart/End	213,247
Multiplier	31789.56355
% Difference	0.752209444

Figure 34: Low Background C Subtraction

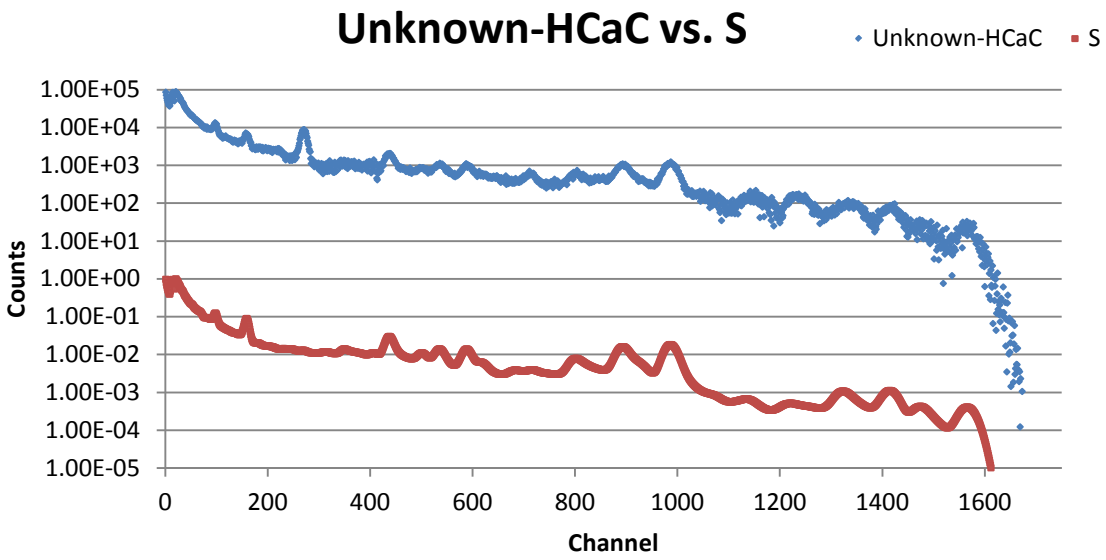

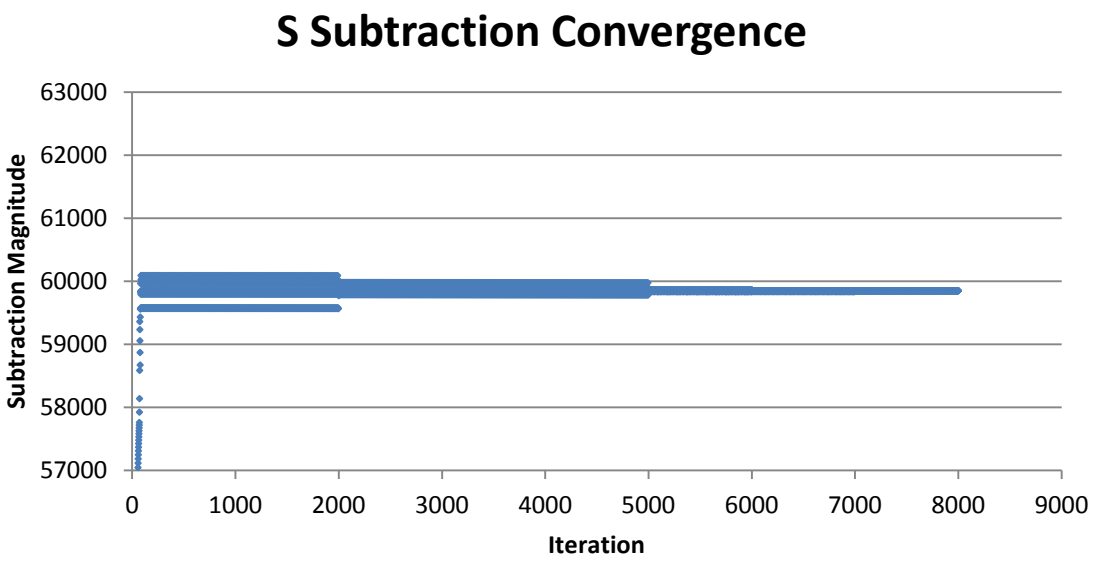

Chisquared	34.3053
SubStart/End	138,170
Multiplier	59859.07743
% Difference	1.413472889

Figure 35: Low Background S Subtraction

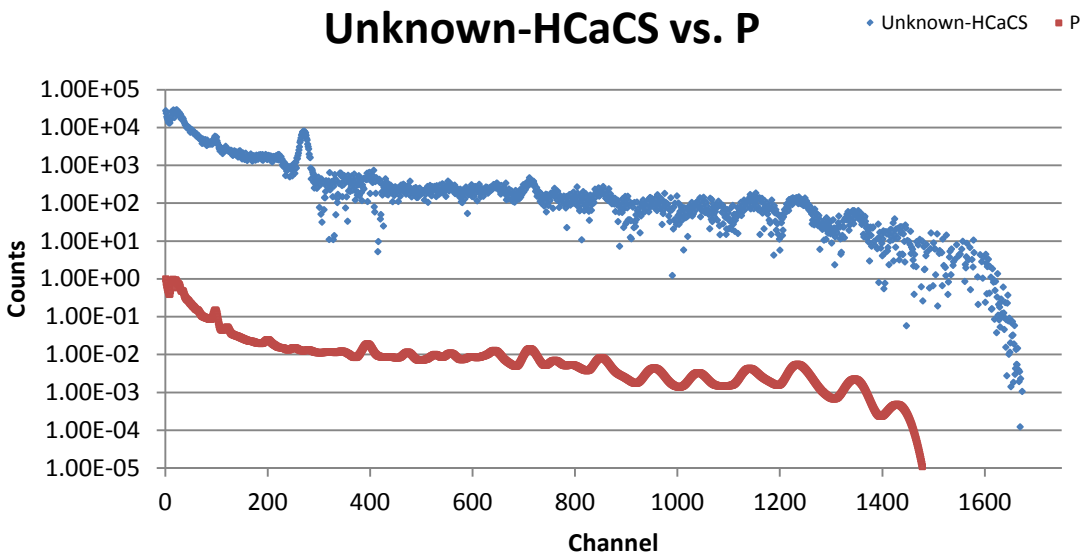

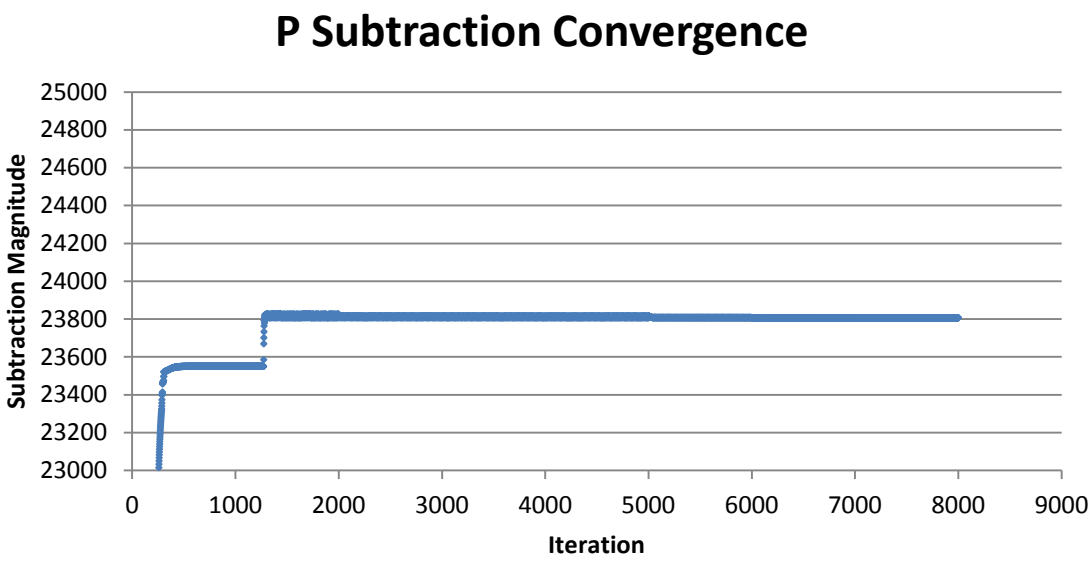

Chisquared	33.3239
SubStart/End	685,742
Multiplier	23808.04037
% Difference	3.026753532

Figure 36: Low Background P Subtraction

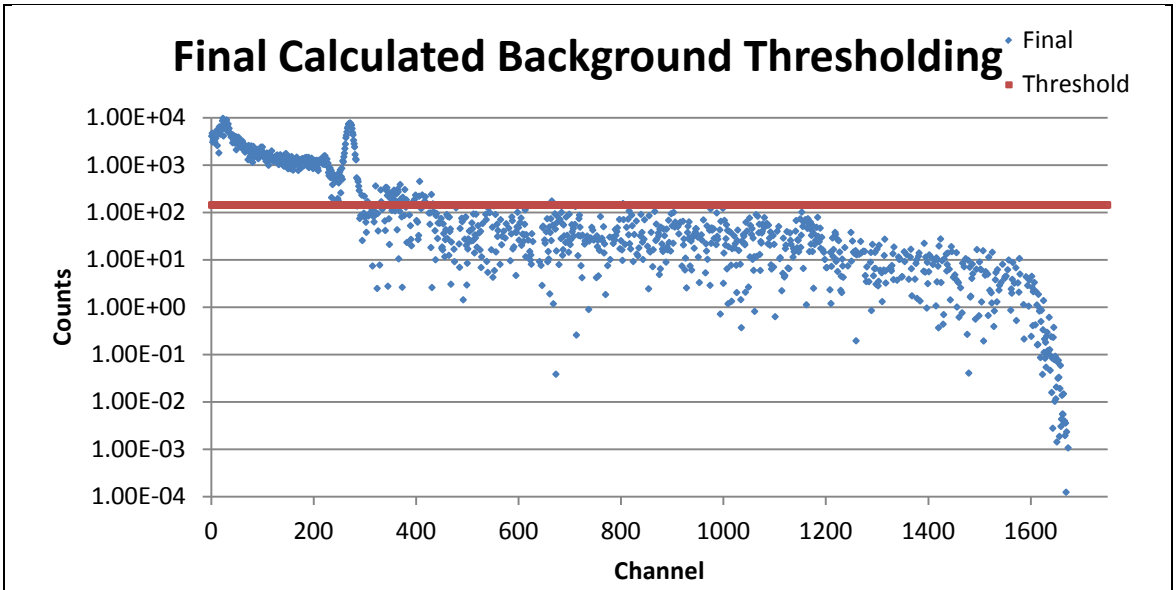

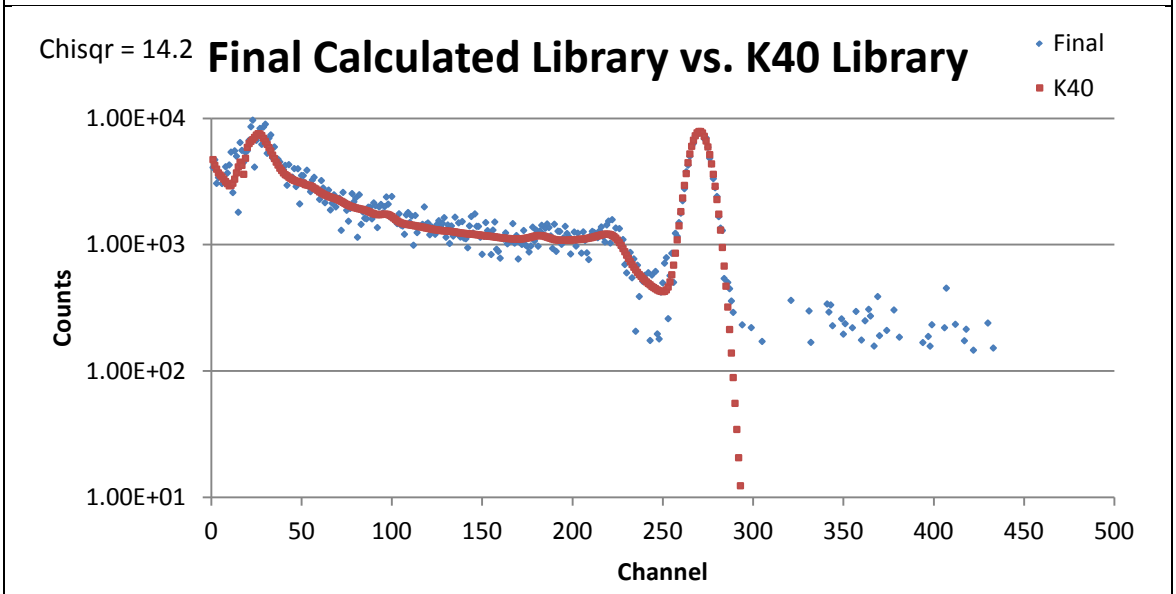

Library	LLS Multiplier w/o Bkgd	LLS Multiplier with Bkgd	% Difference w/o Bkgd	% Difference with Bkgd
H	652655	626536	4.029653763	0.133572638
Ca	24986.6	24894.7	0.9501988	1.314501136
C	32635.2	32108.5	1.887888107	0.243517897
S	59639	59811.9	1.775935359	1.491173026
P	23181.9	23251.9	0.317197926	0.620115455

Figure 37: Low Background Final Calculated Library Comparison to True Background Library

Convolved Peak Subtraction Method Applied to Low Background Artificial Spectrum

To further demonstrate the effect a lower missing library contribution can have on the subtraction method, the convolved peak demonstration detailed in the previous section will be repeated on the unknown shown in Figure 31. The convolved peak subtraction will again operate on a convolved peak that exists between carbon and sulfur, and will proceed in the same way as previously described. Figure 38 shows the results of the convolved peak subtraction method, and Figure 39 shows the resulting calculated library alongside its effectiveness at improving a library least-squares fit. These results will be reported in the same way as in previous sections.

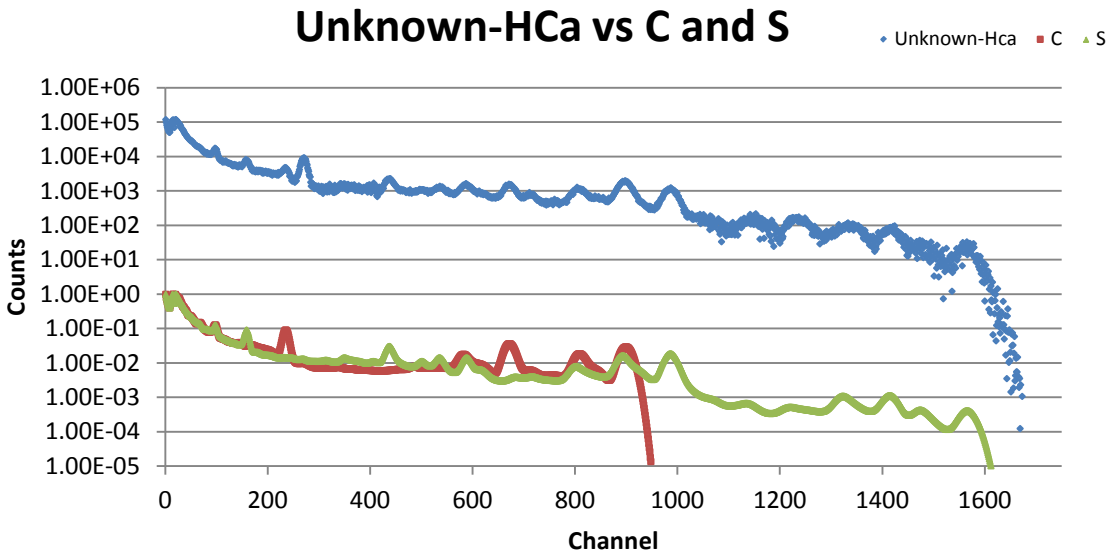

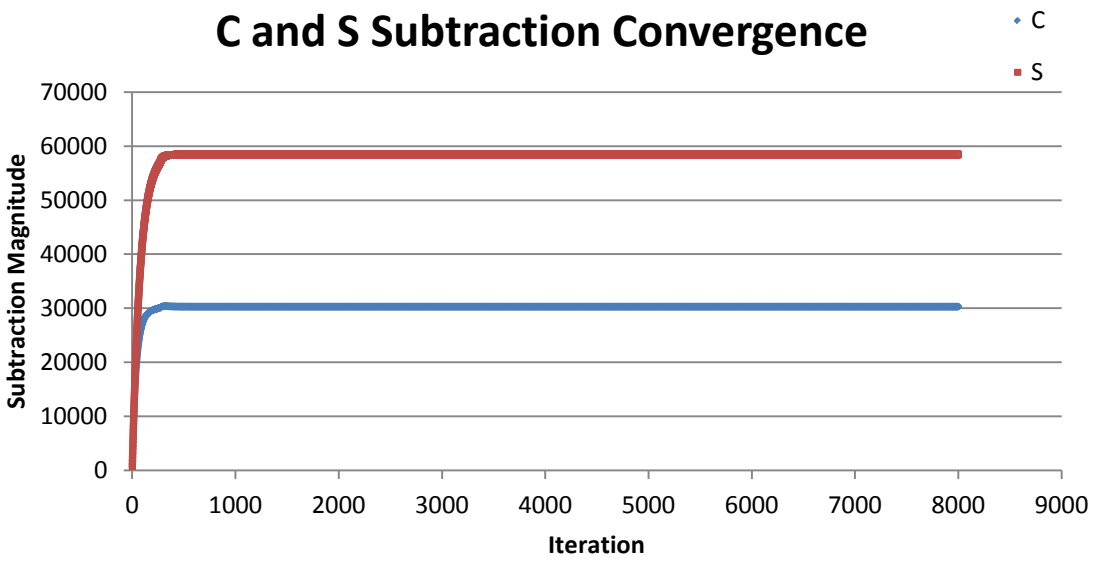

Chisquared	26.965
SubStart/End	860,950
C Multiplier	30331.32
S Multiplier	58463.65
C % Difference	5.304883
S % Difference	3.711704

Figure 38: Low Background C and S Convolved Subtraction

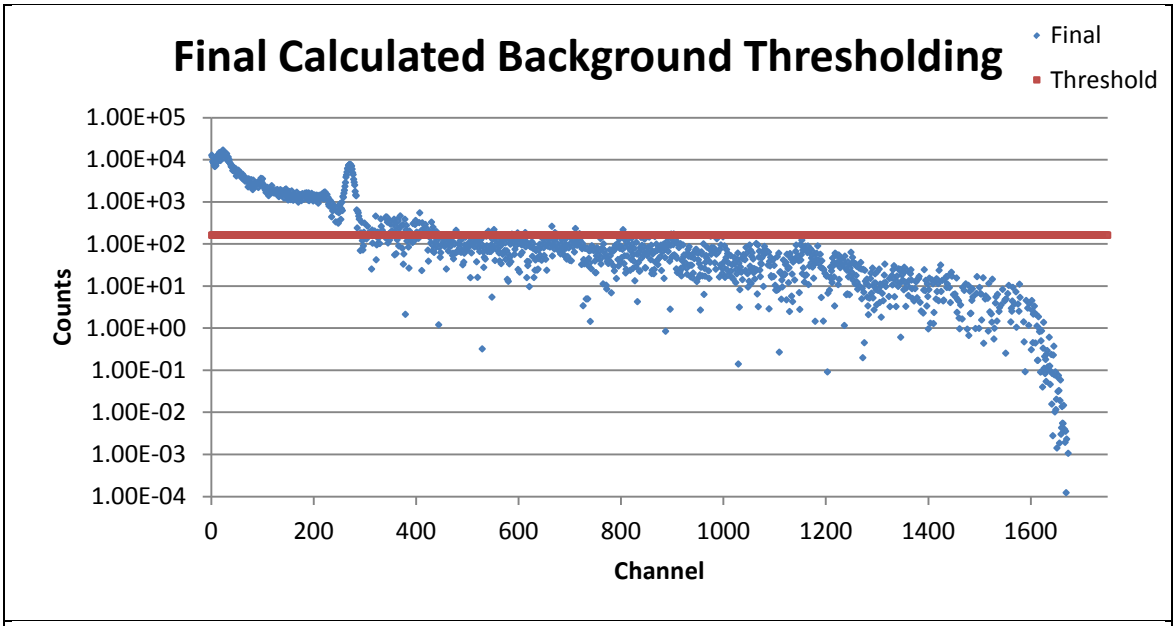

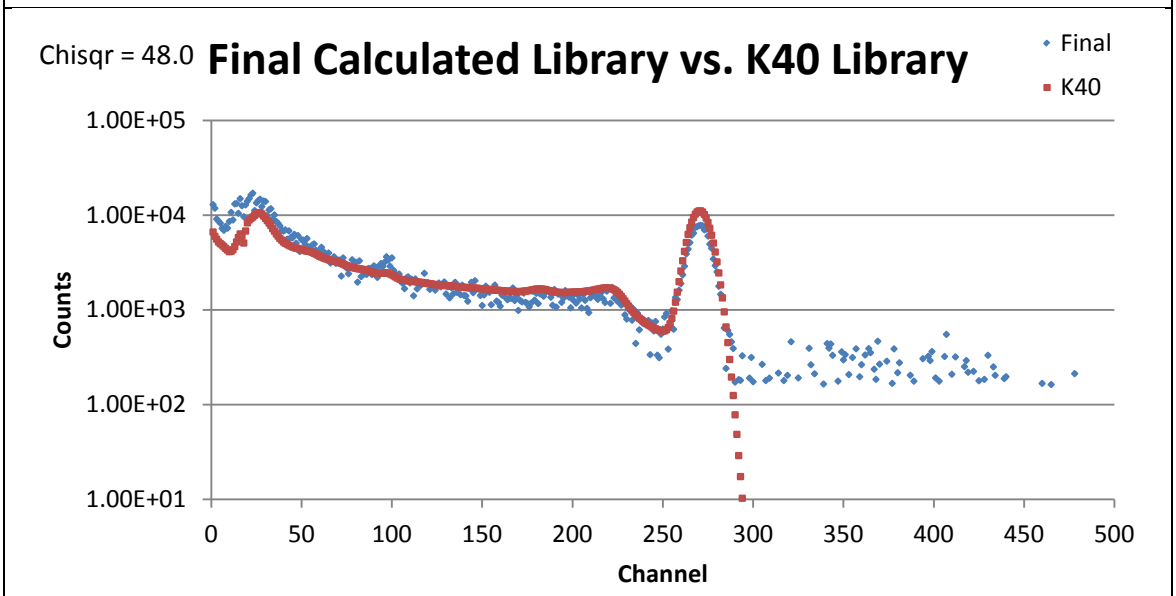

Library	LLS Multiplier w/o Bkgd	LLS Multiplier with Background	% Difference w/o Bkgd	% Difference with Bkgd
H	652655	622063	4.029653763	0.846544485
Ca	24986.6	25035.8	0.9501988	0.755164253
C	32635.2	31565.4	1.887888107	1.452053511
S	59639	59398.5	1.775935359	2.172033341
P	23181.9	23019.2	0.317197926	0.386868958

Figure 39: Low background Final Calculated Library Comparison to True Background Library, Convolved

Real Spectrum Analyzed by Iterative Single Peak Subtraction

The previous sections show the viability of this subtraction method on the artificial spectrum created as described in earlier sections. To demonstrate this method on a real spectrum, a simple experiment was devised. A measurement will be taken of three button sources by a sodium iodide (NaI) scintillation detector. The collected spectrum will not solely be the result of these three radionuclides. Several sources of background radiation will also contribute to the final spectrum. These range from radioactive elements in the building materials to radioactive elements in the soil. In addition to these natural sources of background there is a large amount of fertilizer stored in the room this spectrum will be taken in, giving rise to a large potassium peak. In keeping with the artificial spectra tests, the goal of subtraction on this real spectrum will be to reproduce the shape of the background present in the unknown. The three button sources will act as the known libraries. As computational libraries are not available for this detector setup, experimental libraries will be obtained. These libraries must be free of the background present in the unknown spectrum, so the background in these library spectra will be removed prior to the iterative subtraction of the unknown. A picture of the detection system can be found below in Figure 40.

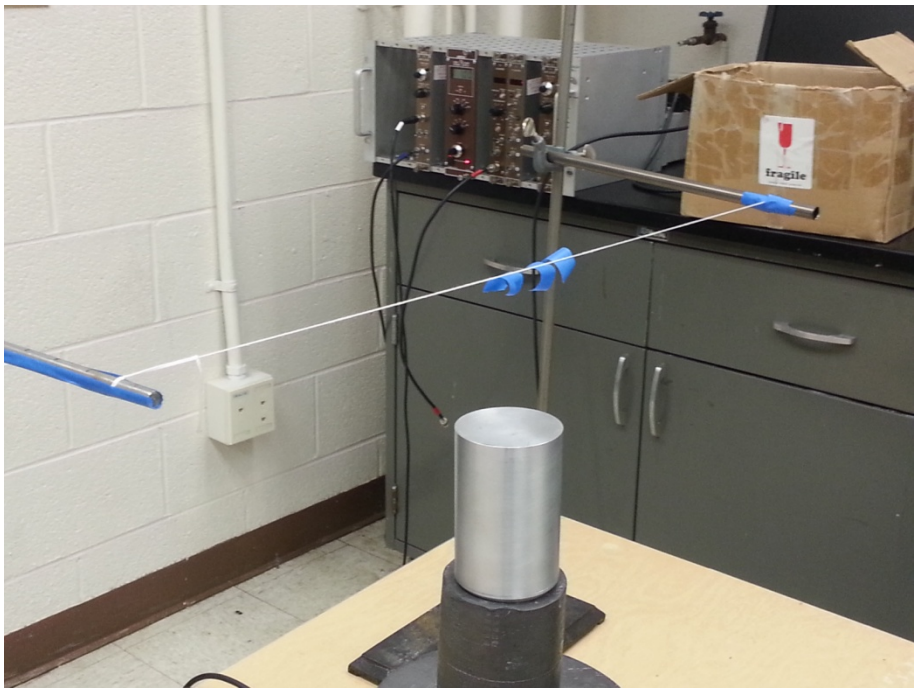

Figure 40: Detection System

The creation date, initial activity, and activity at the time of the experiment can be found in Table 9.

Table 9: Button Source Information

Source	Creation Date	Initial Activity (μCi)	Half Life (Months)	Current Activity (μCi)
Co60	May-01	1	63.2523	6.030345023
Cs137	May-01	1	362.04	1.368781754
Ba133	May-01	1	126.12	2.462413015

Collected Spectra

All spectra displayed in this section have a collection time of one hour and utilize the experimental setup detailed in the previous section. The background spectrum collected in this experiment is shown below in Figure 41.

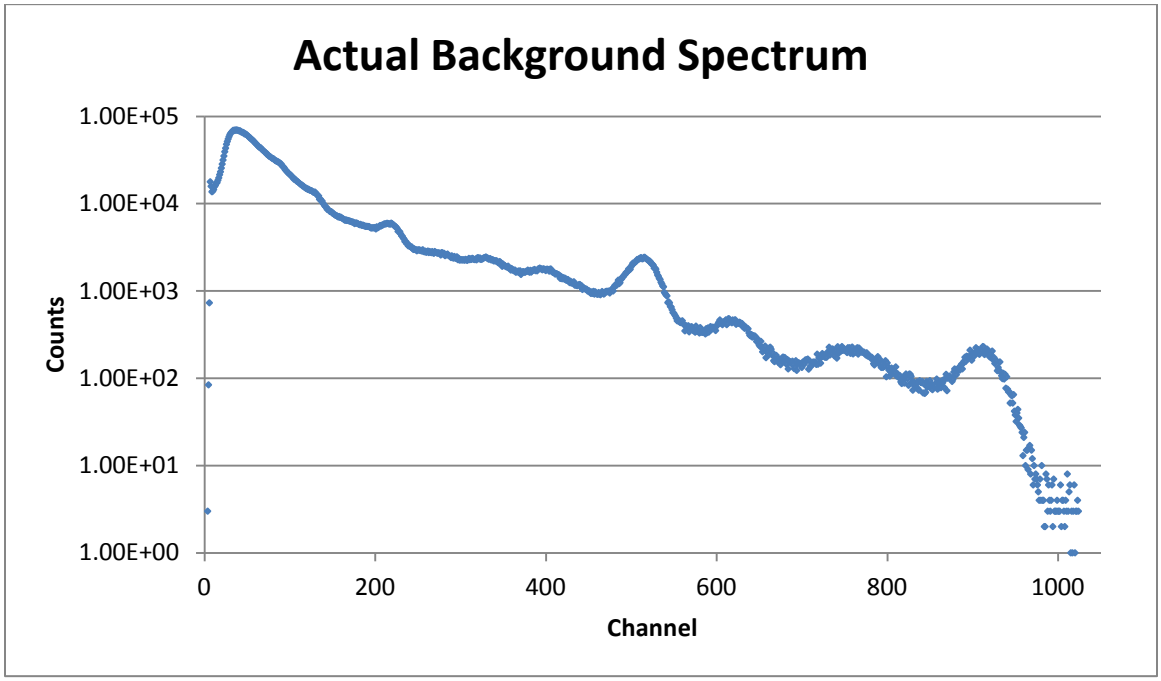

Figure 41: Actual Background for Experimental Spectrum

This spectrum is what the iterative subtraction method hopes to reproduce, and what the residual spectrum calculated by the method will be compared against. Figure 42 below is the combined spectrum of all the button sources as well as the background spectrum shown above. This spectrum will be the initial input for the subtraction method and as such will have all of the following libraries subtracted from it.

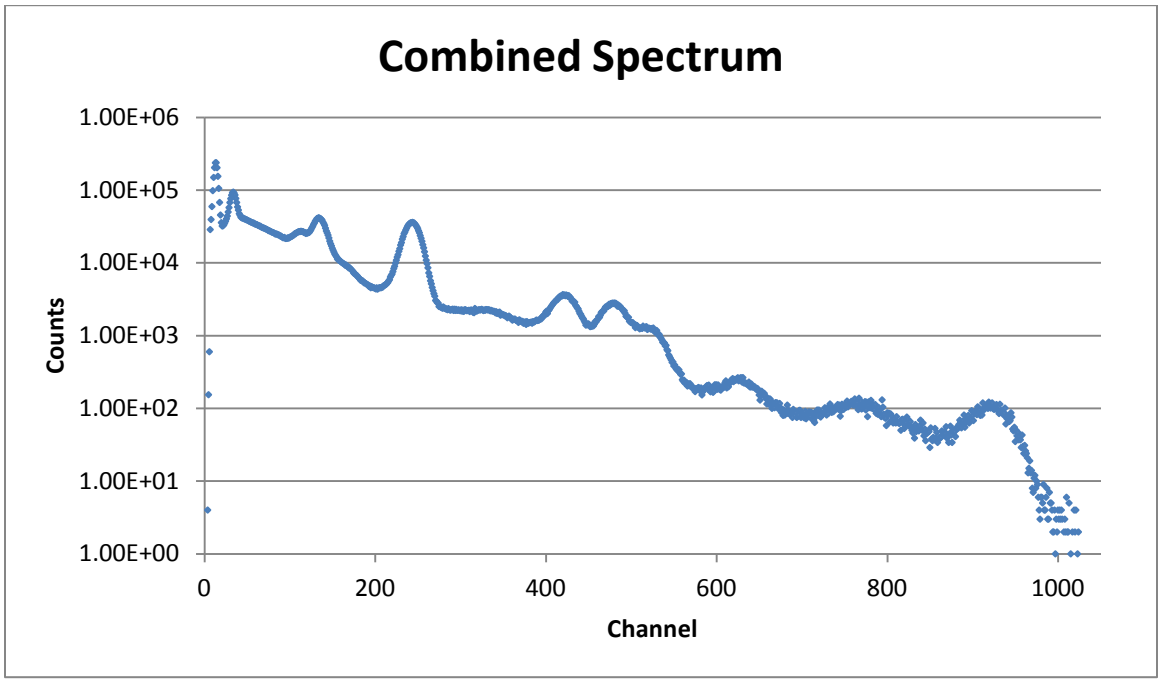

Figure 42: Spectrum of all three Button Sources and Background

Figure 43 through Figure 45 show the collected library spectra as well as the residual from the subtraction of the background spectrum in Figure 41. This residual represents the one hour contribution of the source to a spectrum that it is a part of. These libraries were normalized to their highest values before the subtraction method was performed, as the libraries used in the artificial spectra were normalized. The normalization constant for each library is reported in Table 10, and will represent the true multiplier for each library that this method will hope to reproduce.

Table 10: Normalization Constants for Experimental Libraries

Source	Multiplier
Ba133	182422
Co60	3013
Cs137	30128

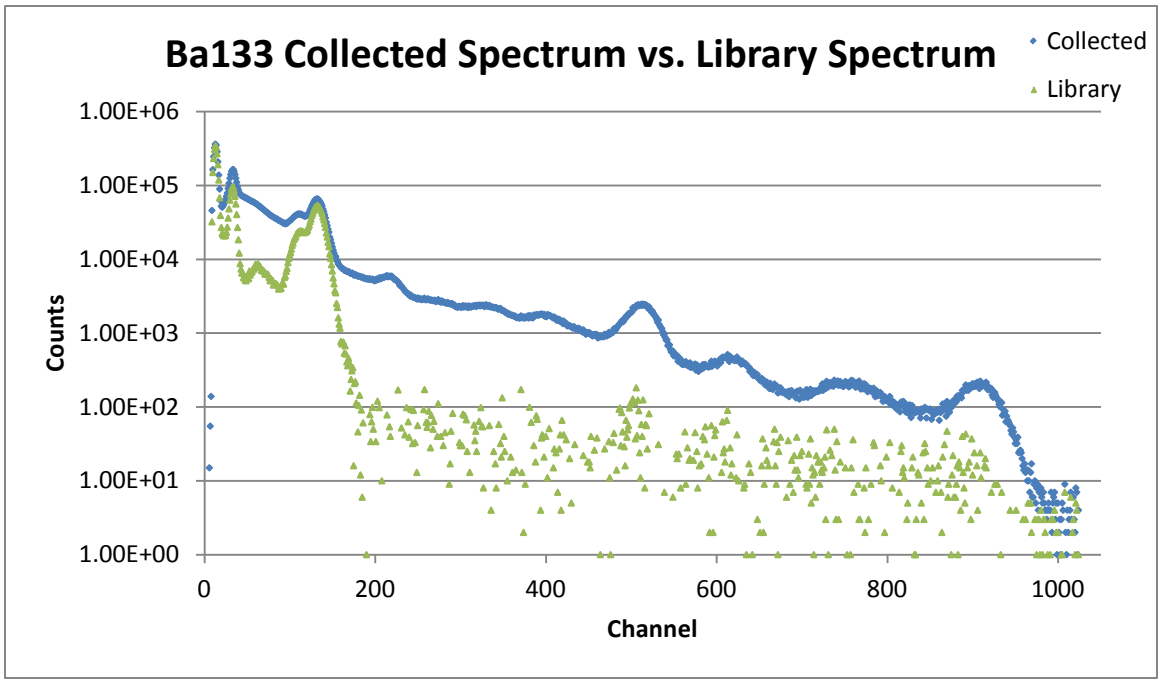

Figure 43: Collected Spectrum of Ba133 compared to Library Spectrum of Ba133

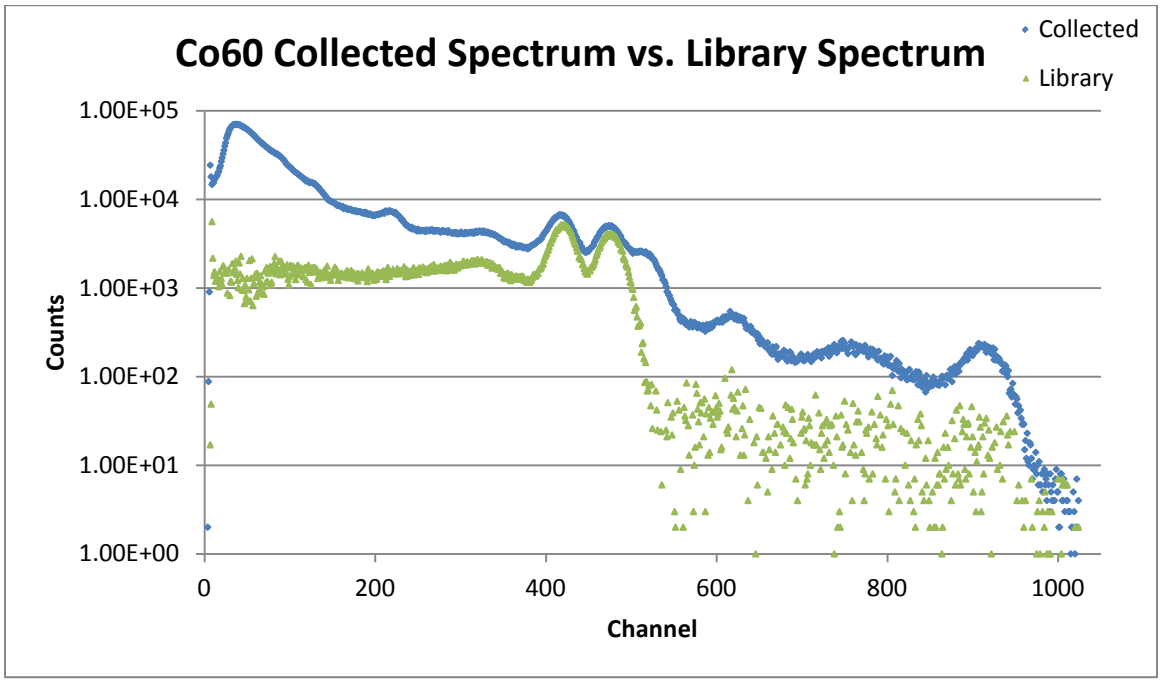

Figure 44: Collected Spectrum of Co60 compared to Library Spectrum of Co60

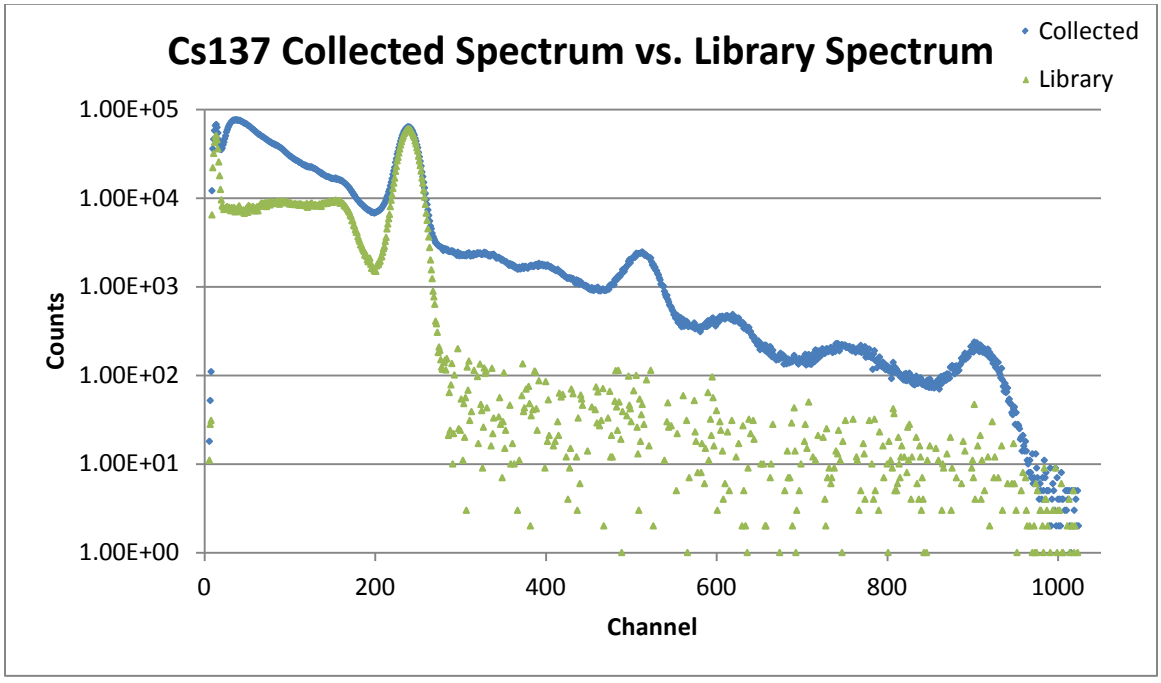

Figure 45: Collected Spectrum of Cs137 compared to Library Spectrum of Cs137

Iterative Single Peak Subtraction of Combined Experimental Spectrum

Figure 46 through Figure 48 show the results of subtracting the library spectra shown in Figure 43 through Figure 45. The results of these subtractions will be reported in the same way as in the previous sections.

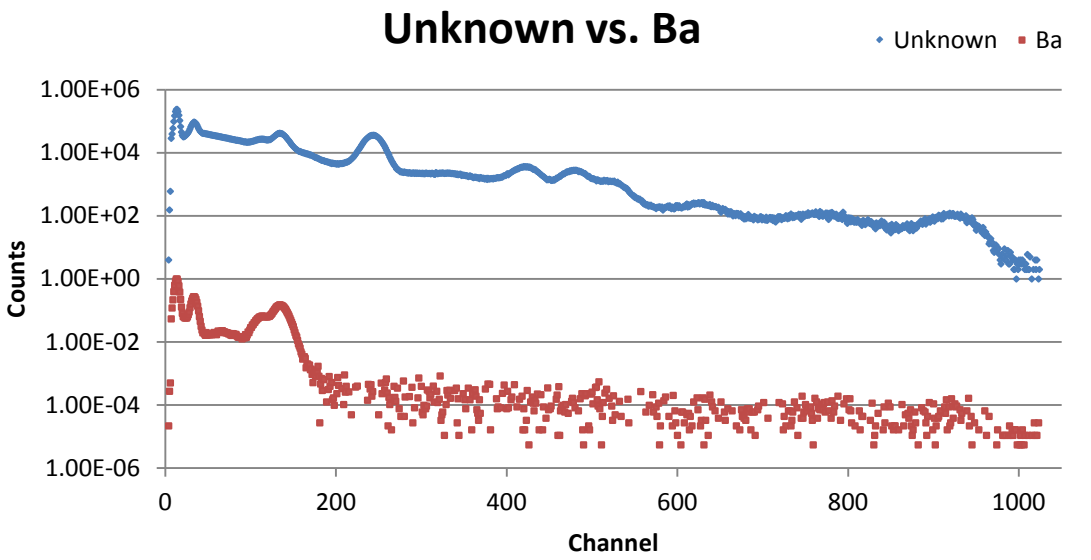

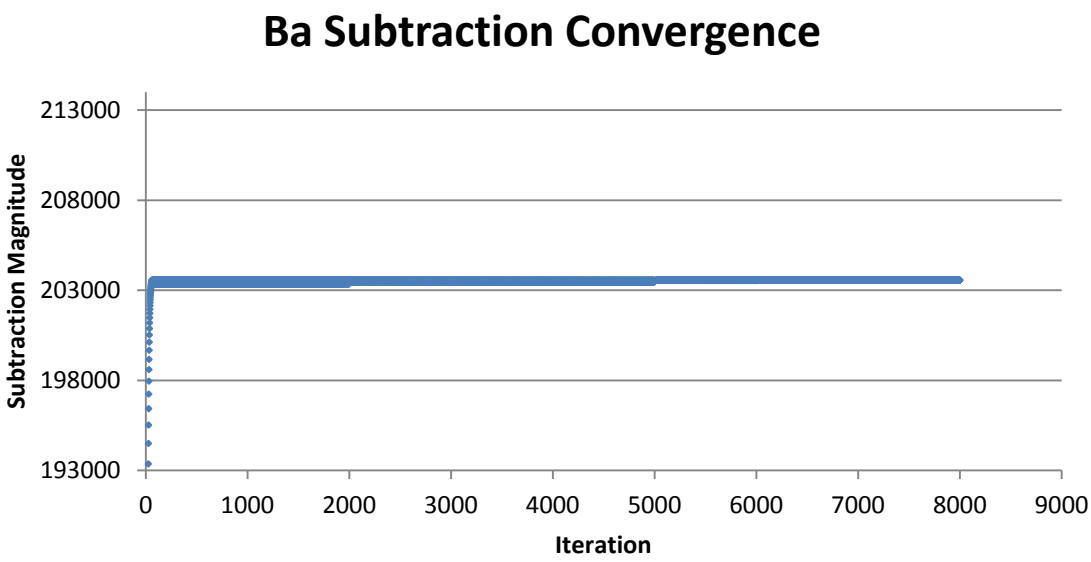

Chisquared	7.4219
SubStart/End	122,145
Multiplier	203570.2734
% Difference	11.59178

Figure 46: Experimental Spectrum Ba Subtraction

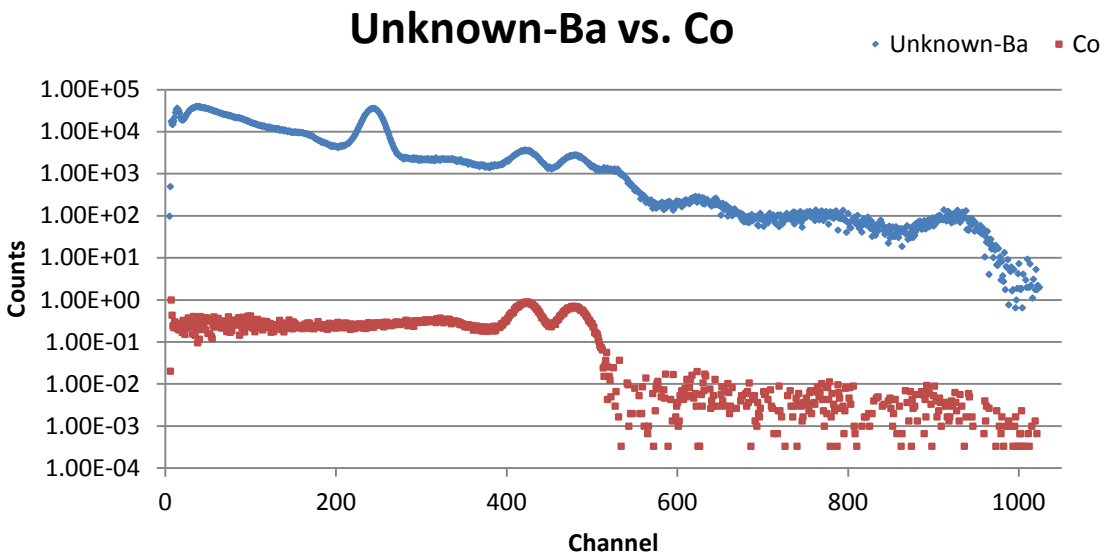

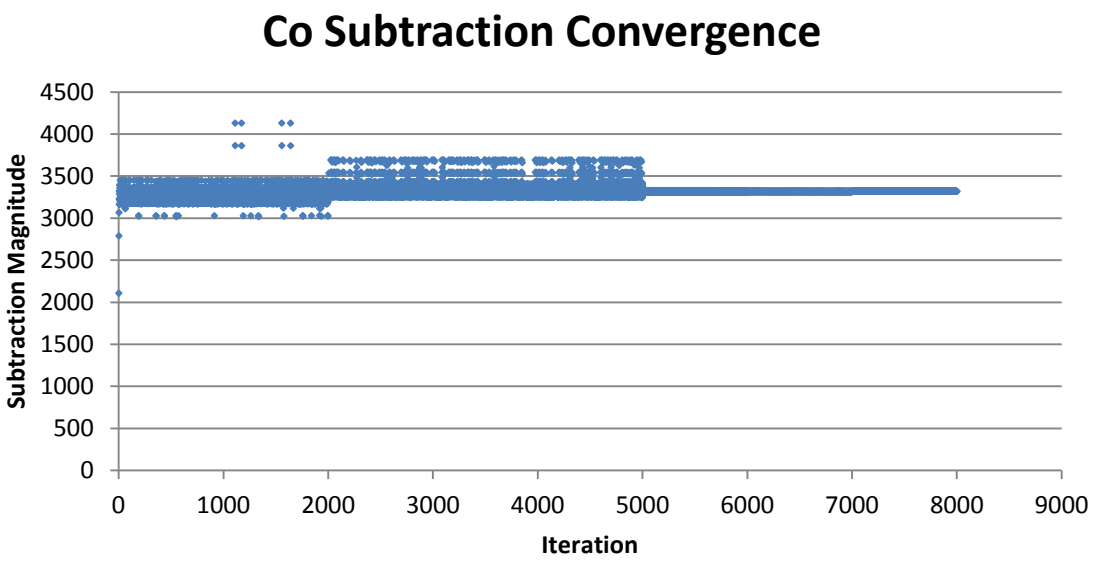

Chisquared	14.0992
SubStart/End	400,445
Multiplier	3323.710852
% Difference	10.31234

Figure 47: Experimental Spectrum Co Subtraction

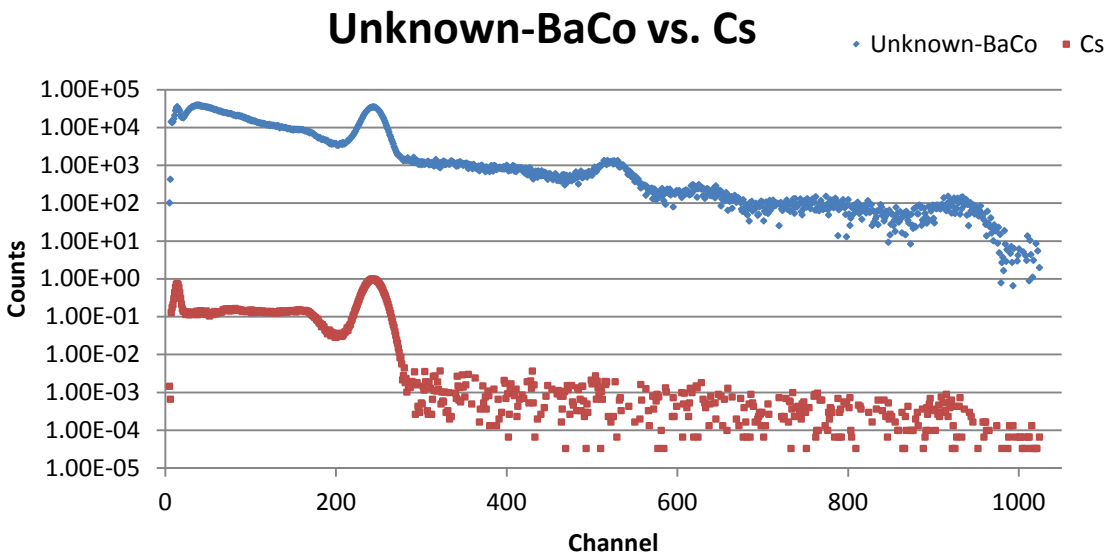

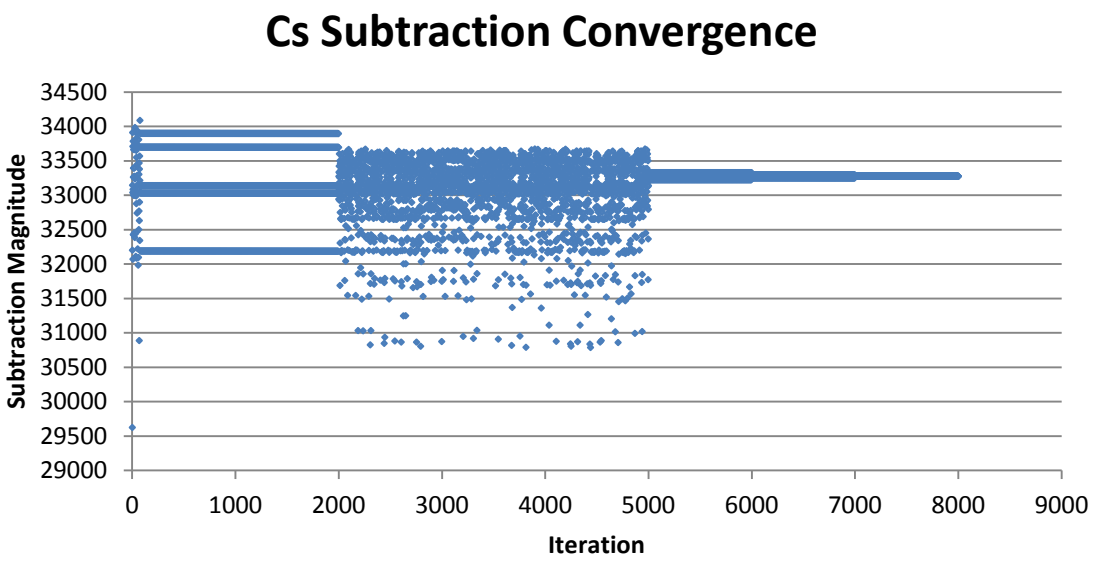

Chisquared	63.4028
SubStart/End	231,261
Multiplier	33281.22693
% Difference	10.4661

Figure 48: Experimental Spectrum Cs Subtraction

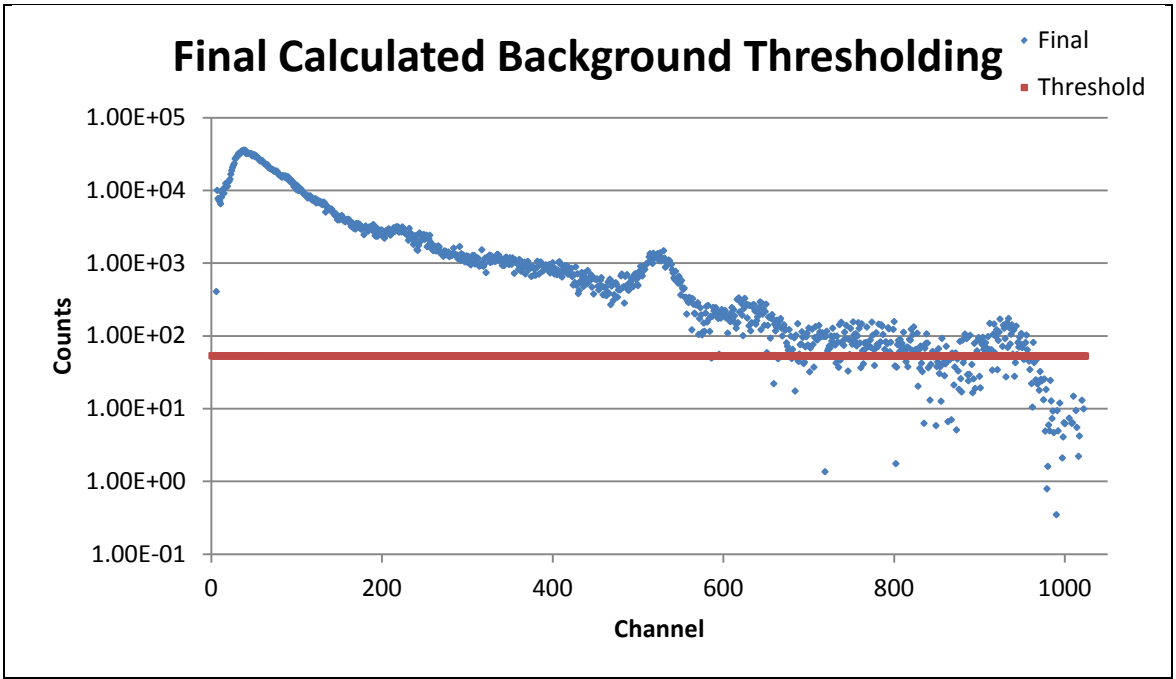

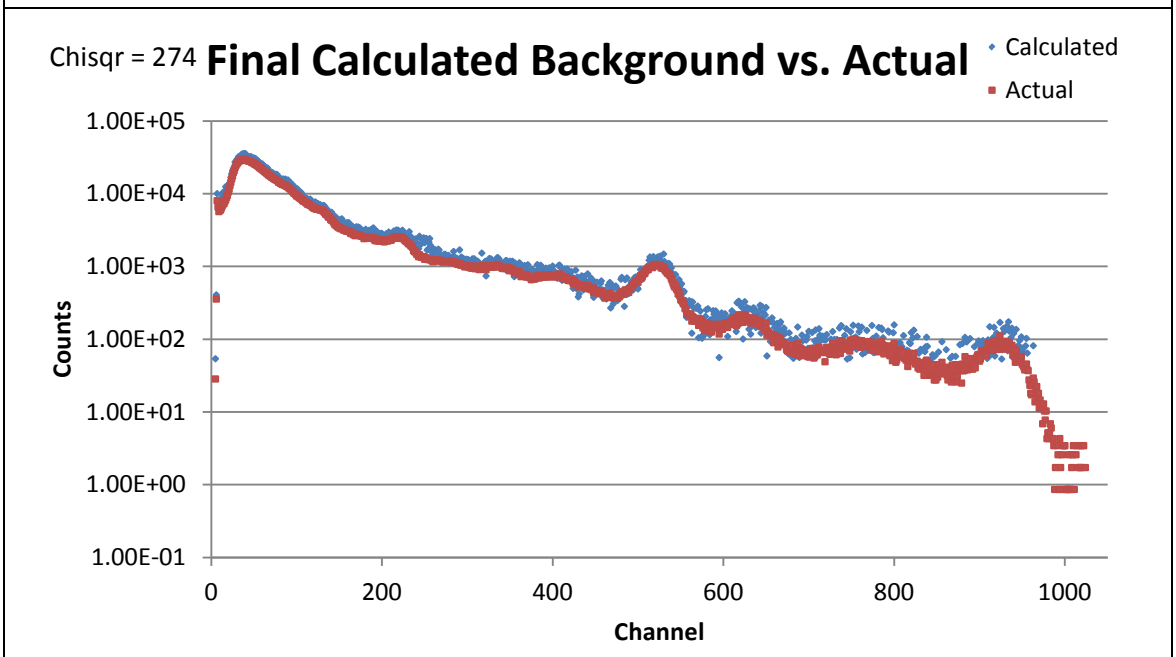

Library	LLS Multiplier w/o Bkgd	LLS Multiplier with Bkgd	% Difference w/o Bkgd	% Difference with Bkgd
Ba133	308703	203365	69.22465492	11.48052318
Co60	5487.57	3322.63	82.12977099	10.27646864
Cs137	45168.5	33261.7	49.92199947	10.40128784

Figure 49: Experimental Spectrum Final Calculated Library Comparison to True Background Library

Discussion of Results

Artificial Single Peak Subtraction Process

For the purposes of this discussion refer to Figure 23 through Figure 27 as well as Figure 32 through Figure 36. These figures show the necessity of the dampening scheme detailed in previous sections. The behavior from iterations 1-2000 show the behavior of the subtraction process with no dampening, and for several of these libraries convergence simply would not happen without external measures. However, the application of the dampening scheme resulted in satisfactory convergence in all cases. Observation of the indicated figures will show that the convergence behavior differed from isotope to isotope, sometimes drastically. Even the same isotope can exhibit different convergence behavior across the two different test cases; the Ca library is an example of this.

The final chi-squared of the model's fit across the indicated peak area can be found below in Table 11 as well as the percent differences between the final multiplier and the true multiplier.

Table 11: Artificial Spectrum Single Peak Subtraction Metrics

Library	High Bkgd ChiSqr	Low Bkgd ChiSqr	High Bkgd % Diff	Low Bkgd % Diff
H	146.8367	39.9984	0.128	0.131
Ca	23.7826	19.8109	0.73033	6.864
C	5.7639	21.3472	2.8266	0.752209
S	3.9917	34.3053	2.6779	1.4134
P	36.857	33.3239	2.9467	3.0267535

The percent differences obtained for both cases are very favorable, showing a close agreement with the true values. Perhaps most importantly, the deviation from the true value does not seem to be a function of the order of subtraction; instead the counting statistics of the peak operated on play a greater part. This fact alone would suggest an improvement over the spectral stripping method. In both cases the chi-squared for the final H library subtraction was the highest. This can be explained by a mild convolution with a peak in the Ca library. However, there does not appear to be a relationship between the chi-squared value of the model fit on convergence and the accuracy of the multiplier obtained. This means that the chi-squared value of the subtraction method can only be used to determine when the subtraction has reached a local minimum rather than as an indicator of the quality of the library multiplier found.

Artificial Convolved Peak Subtraction Process

For the purposes of this section refer to Figure 29 and Figure 38. The convergence of the convolved peaks differed from their singly subtracted counterparts. The convolved subtraction converged before the dampening scheme constants were applied, whereas the singly subtracted peaks needed the full extent of the dampening scheme to reach convergence. This is most likely due to the parameters that have been fixed in the convolved model. As the solver does not need to search for nonlinear parameters convergence is much easier to achieve.

Table 12 shows the solved multipliers for the convolved peak operated on as well as the corresponding values determined by single peak subtraction.

Table 12: Comparison of Convolved to Single Multipliers

High Background			
Library	Single Sub Multiplier	Convolved Multiplier	True Multiplier
C	31125.1014	29965.79	32030.5
S	59091.34	61109.78	60717.3
Low Background			
Library	Single Sub Multiplier	Convolved Multiplier	True Multiplier
C	31789.56355	30331.32	32030.5
S	59859.07743	58463.65	60717.3

In all cases but the high background S multiplier the single peak subtraction method gave a more accurate result. The convolved multipliers are still reasonable approximations of the true multiplier; the highest percent difference when compared to the true value is below 7%.

Experimental Spectrum Single Peak Subtraction

Refer to Figure 46 through Figure 48 for this section's discussion. The convergence behavior displayed similar characteristics to the artificial subtraction convergence. Once again, satisfactory convergence would not have been achieved without the application of the dampening scheme. The percent difference between the "true" values and the calculated ones, while higher in magnitude, do not greatly change due to successive subtractions. This would indicate that any error present in the value obtained is not due to the successive nature of the subtraction, unlike spectral stripping.

Threshold application and True Library Comparison

Refer to Figure 28, Figure 30, Figure 37, Figure 39, and Figure 49 for the purpose of this discussion. The application of the threshold and subsequent comparison to the true

background in the high background single subtraction case resulted in chi-squared value of 0.86, which suggests a good fit. The large number of counts this library likely contributed to this low chi-squared value, as there was very good counting statistics in the range this library was present in. That being said, the resulting fit from the low background single subtraction background library resulted in a chi-squared of 14.2, which is still a good result. The convolved spectra had more varied results. The high background convolved subtraction case resulted in chi-squared fit to the true background that mirrored the single peak high background case. The low background convolved subtraction case resulted in a chi-squared value that was much higher than the single peak analysis of the same case. The most likely reason for this discrepancy is the error present in the S library magnitude the convolved method resulted in; the magnitude of the S library is much greater than the C library so greater percent differences will be more evident in the final solution. The experimental spectrum shows the first failure of the threshold method. The shape of the background in the experimental spectrum is much different than in the artificial spectra; as it covers a greater range of channels than the K40 library there are more likely to be spectra features at high energies at lower counts. The threshold applied to the calculated background library for the experimental spectrum is too high and cuts off features of the background unnecessarily. As a result, the fit of the true background to the calculated one is poor.

LLS Multiplier Comparisons with and without Calculated Background Library

Refer to Figure 28, Figure 30, Figure 37, Figure 39, and Figure 49 for the purpose of this section. Table 13 below shows the chi-squared values of the library least-squares (LLS) fit of the unknown for each case with the calculated background library and without it.

Table 13: LLS Case Comparison Values

Case	ChiSqr
High, Single, No Bkgd	197.777
High, Single, Bkgd	1.3446
Low, Single, No Bkgd	8.7064
Low, Single, Bkgd	1.1764
High, Convolved, No Bkgd	197.77
High, Convolved, Bkgd	1.3446
Low, Convolved, No Bkgd	8.7064
Low, Convolved, Bkgd	1.1605
Exper, No Bkgd	397.308
Exper, Bkgd	3.63364

In every case using the calculated background library greatly decreased the chi-squared value of the LLS. The use of a convolved peak did not affect the chi-squared value of the fit in any appreciable way. Even with a bad threshold on the experimental spectrum, enough of the shape of the true background remained to get a good fit to the experimental spectrum. The percent differences between the LLS values for the multipliers and the true value for the multipliers also show the same trend; the values improve or remain the same at worst.

Conclusions

It would seem that on an individual subtraction level the chi-squared value of the model's fit is not a relevant metric to determine the accuracy of the subtraction. Instead it falls to the operator of the program to determine if the subtracted amount seems reasonable. As long as peaks are chosen that are not heavily convolved with the unknown library, it should be

evident if the peak being operated on is gone and replaced with only a continuum. However, unaccounted for convolution could result in an over subtraction that an operator would be harder pressed to notice. That being said the iterative subtraction method resulted in close fits to the true values for each library, with a maximum percent difference between the calculated and true value found in the experimental dataset at 11%.

Convergence using only CURMOD is not always assured, as the initial iterations of subtraction show. However, by using the dampening scheme outlined in this paper, convergence can be achieved in all cases. The validity of the convergence, however, will come down to the operator inspecting the residual spectrum for anomalies both inside the former peak range and elsewhere in the spectrum. If a large enough error exists, other sections of the spectrum may bear divots where none should exist.

The threshold method for removing noise in the calculated background library had mixed results. For a missing background library of low energy, such as K40, the threshold was sufficient to remove the noise in front of where the true library ends. This resulted in very good fits in all of the artificial cases. However, when faced with a background spectrum like the one found in the experimental case, the threshold was set too high. This caused the loss of real spectral information in the calculated library and resulted in a poor fit to the true library.

In all cases, performing this method on a spectrum that contained a source of radiation not accounted for by the libraries at hand improved the library least-squares fit of the known libraries to the unknown spectrum they were applied to. Even in the experimental case, with

its poor fit to the true background, enough of the background shape remained to resolve the known libraries close to their true value.

The purpose of this work was to improve upon the spectrum stripping method by adding the capability to approximate the spectral shape of radioisotope sources not accounted for in the user's array of libraries. The results presented in the previous sections show that the iterative subtraction method improves upon the accuracy of the spectral stripping method by operating in areas with better counting statistics. The results also show that through iterative subtraction an approximation of missing libraries can be calculated and utilized in a library least-squares fit successfully.

Future work

Alternative solvers could be investigated to find one that can better handle the convergence of this method. The dampening scheme worked well enough, but it adds another layer on top of a laborious process. Finding a solver that was capable of converging without any coaxing would simplify the method. The peak fitting model could be greatly expanded on. The approximation of a full energy peak as a Gaussian function is very simplistic; peaks of this nature deviate from Gaussian behavior primarily in the low energy half of the peak in the form of tailing. The model for the continuum is also very simplistic. While it worked well enough during the development of this method, improving the model could very well lead to easier convergence as well as more accurate results. Finally, a new method of determining which portions of the calculated background library are actual spectral features will need to be developed. The threshold method employed in this work is a very crude way of dealing

with the problem; if this method is to be applied to more complex spectra with more complex missing libraries, the threshold method will not produce accurate results. Data smoothing or thresholds set at a rolling average could be possible alternatives to consider moving forward.

Works Cited

Bevington, P. R. (2003). *Data Reduction and Error Analysis.* New York: McGraw-Hill.

Box, G. M. (1958). A note on the generation of random normal deviates. *Annals Math. Stat., 29*, 610-611.

DiNova, V. (2011). Automated Spectrum Stripping of Photon Spectra. *MS Thesis; North Carolina State University*.

Furr, A. (1968). A Spectrum Stripping Technique for Qualitative Activation Analysis Using Monoenergetic Gamma Spectra. *Nuclear Instruments and Methods, 63*, 205-209.

Gardner, R. (1997). Single Peak Versus Library Least-Squares Analysis Methods for PGNAA Analysis of Vitrified Waste. *Applied Radiation and Isotopes, 48*, 1331-1335.

Gardner, R. P. (2004). A Monte Carlo simulation approach for generating NaI detector response functions (DRFs) that accounts for non-linearity and variable flat continua. *Nuclear Instruments and Methods in Physics Research , B 213*, 87-99.

Han, X. (2007). CEARCPG: A Monte Carlo Simulation Code for Normal and Coincidence Prompt-Gamma Ray Neutron Activation Analysis. *Nuclear Science and Engineering, 155*, 143-153.

Knoll, G. F. (2010). *Radiation Detection and Measurement.* Hoboken: John Wiley & Sons.

Krane, K. S. (1988). *Introductory Nuclear Physics.* Hoboken: John Wiley & Sons.

Marquardt, D. W. (1963). An Algorithm for Least-Squares Estimation of Nonlinear Parameters. *Journal of the Society for Industrial and Applied Mathematics, 11*(2), 431-441.

Mitchell, D. J. (2008). *Calculation of Background Radiation for Gamma-Ray and Neutron Detectors.* Albuquerque: Sandia National Laboratories.

Routti, J. (1969). Photopeak Method for the Computer Analysis of Gamma-Ray Spectra from Semiconductor Detectors. *Nuclear Instruments and Methods, 72*, 125-142.

Salmon, L. (1961). Analysis of Gamma-Ray Scintillation Spectra by the Method of Least Squares. *Nuclear Instruments and Methods, 14*, 193-199.

Sood, A. (2004). A new Monte Carlo assisted approach to detector response functions. *Nuclear Instruments and Methods in Physics Research, B 213*, 100-104.